Master's Thesis of Engineering

Development of supraglottic airway device avoiding impairment of carotid artery blood flow

경동맥 혈류 장애를 방지하는 성문위기도기의 개발

February 2018

Interdisciplinary Program in Bioengineering
The Graduate School
Seoul National University
Yoon Ha Joo

경동맥 혈류 장애를 방지하는 성문위기도기의 개발

지도교수 이 정 찬

이 논문을 공학석사학위논문으로 제출함

2017년 12월

서울대학교 대학원

협동과정 바이오엔지니어링

주윤하

주윤하의 석사학위논문을 인준함

2018년 1월

위 원 장 김 희 찬 (인)

부 위 원 장 이 정 찬 (인)

위 원 최 영 빈 (인)

Development of supraglottic airway device avoiding impairment of carotid artery blood flow

*Academic adviser*Jung Chan Lee
Submitting a master's thesis of Engineering
January 2018

Interdisciplinary Program in Bioengineering
Graduate School, Seoul National University

Yoon Ha Joo

Confirming the master's thesis written by Yoon Ha Joo
January 2018

Chair _____
Hee Chan Kim, Ph.D.

Vice Chair _____
Jung Chan Lee, Ph.D.

Examiner _____
Young Bin Choy, Ph.D.

Abstract

Development of supraglottic airway device avoiding impairment of carotid artery blood flow

Yoon Ha Joo
Interdisciplinary Program in Bioengineering
Seoul National University Graduate School

The supra-glottic airway(SGA) is a device that have one or two cuffs attached to the end or middle of the tube to cover the larynx. SGA has the advantages of simple configuration and relatively low skill required. So, this is the most popular alternative to endotracheal intubation(E-tube intubation) and has already been widely introduced in medical practice. However, recent large-scale studies of patients with cardiac arrest in out of hospital have reported that SGA intubation have worse spontaneous circulation recovery, survival rate, and neurological prognosis than E-tube intubation. It is presumed that the pressure of the laryngeal lumen which occurs when the cuff inflated on the glottis is closely attached to the airway entrance obstructs the blood flow of the carotid artery but not proved yet. The purpose of this study is to identify what differences are occurring and analyze the causes of various types of SGAs and E-tube on hemodynamic aspects and develop of new SGAs that is most advantageous in terms of brain survival in patients with cardiac arrest.

In order to compare with the effects of e-tube and three types of SGAs, laryngeal mask airway(LMA), i-gel and combitube on cerebral

blood flow and pressure, pre-clinical studies were conducted using total of 12 pigs weighing about 40kg cardiac arrest models.

We analyzed the factors affecting the physiological parameters using computed tomography(CT) images of pigs intubated with e-tube and three types of SGAs. First, the 3D model of the SGAs / carotid artery / upper respiratory tract before and after intubation was prepared by Seg3D program , Meshmixerprogram . Second, SGAs after intubation and upper respiratory tract before intubation were output to the FDM 3D printer for detailed appearance analysis. Third, we calculated the volume per unit length of the carotid artery and analyzed whether the carotid artery was pressured by SGAs cuff expansion.

New-LMA and new-combitube were created to reduce the pressure on the carotid artery. This is based on the patent of Earplug US005957136 US4867149, and a plug and plug cuff with thin wings is fabricated using silicone, which is an elastic polymer material. First, a mold was designed to fabricate a cuff using the Inventor program, Seg3D, Meshmixer and outputs using FDM 3D Printer 3DP-110F(Single). Second, a new cuff is fabricated by casting silicon into the mold.

The air-leakage in-vitro test was performed on new SGAs manufactured by using the manikin in the gating system. Preclinical study was conducted on 8 pigs weighing about 42.5kg cardiac arrest model. There was a decrease in carotid artery blood flow in the new-SGA. However, it is confirmed that the decrease is smaller than that of existing products. This allows the new gateways to demonstrate improved performance over existing products.

Keywords : supraglottic airway(SGA), computed tomography(CT) analysis, 3D modeling, 3D printing
Student Number : 2016-21179

Table of Contents

Abstract ····· iv

List of Tables ····· viii

List of Graph ····· viii

List of Figures ····· ix

Chapter 1. Introduction ····· 1

Chapter 2. Method ····· 71

2.1. Measurement of the effects of the existing-SGA on carotid artery blood flow using animal models ····· 71

2.2. Analysis of blood vessel shape using computed tomography image ····· 91

2.3. Design and manufacture of new-SGA ····· 53

2.4. In-vitro performance evaluation of new-SGAs ····· 25

2.5. In-vivo performance evaluation of new-SGAs ····· 85

Chapter 3. Result ····· 16

3.1. Result of carotid blood flow on existing-SGA intubation using animal model ····· 16

3.2. Analysis of blood vessel shape using computed tomography image ····· 97

3.3. In-vitro performance evaluation of new-SGAs ····· 78

3.4. In-vivo performance evaluation of new-SGAs ····· 98

Chapter 4. Discussion ····· 59

4.1. Discussion of carotid blood flow on existing-SGA intubation using animal model ····· 69

4.2. Discussion of blood vessel shape using computed tomography image ····· 96

4.3. Discussion of new-SGAs ····· 101

Chapter 5. Conclusion ····· 104

Reference ····· 16

List of Tables

Table 1. Analysis of carotid blood flow changes during LMA Intubation ····· 6

Table 2. Comparison of changes in carotid artery blood flow between LMA intubation and EI (baseline) ····· 6

Table 3. Analysis of carotid blood flow changes during IGEL Intubation ··· 6

Table 4. Comparison of changes in carotid artery blood flow between IGEL intubation and EI (baseline) ····· 6

Table 5. Analysis of carotid blood flow changes during combitube Intubation ··· 6

Table 6. Comparison of changes in carotid artery blood flow between combitube intubation and EI (baseline) ····· 6

Table 7. Result of In-vitro performance evaluation about pressure applied to the laryngeal lumen ····· 8

Table 8. Analysis of carotid blood flow changes during existing-IGEL Intubation ··· 9

Table 9. Analysis of carotid blood flow changes during new-IGEL Intubation ··· 9

Table 10. Analysis of carotid blood flow changes during existing-combitube Intubation ····· 9

Table 11. Analysis of carotid blood flow changes during new-combitube Intubation ··· 9

List of Graph

Graph 1. Result of in-vitro performance evaluation of new-SGAs ····· 9

List of Figures

Figure 1. Respiratory system ····· 3

Figure 2. Larynx ····· 4

Figure 3. Positive pressrue ventilation system ····· 7

Figure 4. E-tube ····· 01

Figure 5. EI ····· 01

Figure 6. SGA a) LMA b) IGEL c) combitube ····· 41

Figure 7. Classification of experimental group according to order of airway intubation ····· 81

Figure 8. Preclinical research stage. ····· 81

Figure 9. SI in preclinical studies, ····· 91

Figure 10. Mechanical chest compression CPR in preclinical studies 1

Figure 11. Computed Tomography ····· 22

Figure 12. Brightness change with time after contrast injection ·3····· 2

Figure 13. 3D modeling process ····· 62

Figure 14. 3D modeling process by Seg3D ····· 72

Figure 15. Cropping a) before b) after ····· 82

Figure 16. Filtering a) before b) after ····· 92

Figure 17. Segmentation a) before b) after ····· 03

Figure 18. Paintbrush and polyline function a) before b) after ·1····· 3

Figure 19. 3D models implementation ····· 23

Figure 20. Post-processing ····· 33

Figure 21. Output of FDM 3D printer a) laryngeal lumen before intubation b) SGAs after intubation : LMA (left), combitube(middle), IGEL(right) ····· 43

Figure 22. Multi-flange earplug ····· 34

Figure 23. New-SGAs applying the multi-flange shape a) new-IGEL b) new-combitube ····· 44

Figure 24. Development process of new-SGAs ····· 46

Figure 25. 3D models of new-SGAs a) new-LMA b) new-combitube ····· 47

Figure 26. 3D models of mold a) new-LMA b) new-combitube ····· 48

Figure 27. Molds produced by FDM 3D printer a) mold of new-IGEL b) mold of new-combitube proximal cuff c) mold of new-combitube distal cuff ····· 49

Figure 28. Cuffs of new-SGAs a) new-IGEL cuff b) new-combitube proximal cuff c) mold of new-combitube distal cuff ····· 50

Figure 29. New-IGEL(left) new-combitube (right) ····· 51

Figure 30. In-vitro performance evaluation about sealing. ····· 53

Figure 31. Pressure measuring system applied by SGAs cuff to the laryngeal lumen of the larynx. ····· 55

Figure 32. new-SGAs cuff and silicone cuff made by computerized tomography image of the existing-SGAs a) existing-IGEL cuff b) new-IGEL cuff c) existing-combitube proximal cuff d) new-combitube proximal cuff ····· 56

Figure 33. Measurement of pressure applied by new-SGAs to laryngeal lumen. a) existing-IGEL cuff b) new-IGEL cuff c) existing-combitube proximal cuff d) new-combitube proximal cuff ····· 57

Figure 34. In-vivo performance evaluation of new-SGAs a) new-IGEL b) new-combitube ····· 95

Figure 35. Classification of experimental group according to order of airway intubation ····· 06

Figure 36. Performance evaluation research stage. ····· 06

Figure 37. 3D model of trachea during EI ····· 27

Figure 38. The 3D model of pork laryngeal lumen in the EI ····· 37

Figure 39. 3D model of the laryngeal lumen during LMA intubation 47

Figure 40. 3D model of the laryngeal lumen during IGEL intubation 57

Figure 41. 3D model of the laryngeal lumen during combitube intubation ····· 67

Figure 42. LMA 3D model before and after intubation ····· 87

Figure 43. IGEL 3D model before and after intubation ····· 97

Figure 44. Combitube 3D model before and after intubation ····· 08

Figure 45. Carotid artery 3D model during EI ····· 28

Figure 45. Carotid artery 3D model during LMA intubation ····· 38

Figure 47. Carotid artery 3D model during IGEL intubation ····· 48

Figure 48. Carotid artery 3D model during combitube intubatio 58

Figure 49. Collapsed carotid artery 3D model during combitube intubation ····· 68

Chapter 1. Introduction

1.1. Respiratory system from the anatomical perspective

Respiratory system means a biological system responsible for gas exchange [figure 1]. The respiratory system is divided into upper and lower parts. The upper respiratory system consists of nose, nasal cavity, sinus cavity, pharynx, and larynx. The lower respiratory system, which is described as respiratory tree or bronchial tree, consists of the lower part of the larynx, bronchus, bronchus, bronchi and alveoli [2]. The airway is branched into two main bronchi in the middle of the chest. The bronchus enters the lungs and is progressively branched into narrower secondary and tertiary bronchi, which are branched into multiple bronchioles and eventually associated with alveoli [3, 4, 5, 6]. Gas exchange in the lungs occurs in millions of small air bags called alveoli. Alveoli are fed with abundant amounts of blood, and oxygen is transferred to this blood [1].

The larynx is the organ at the entrance to the airway. [figure 2]. It is located at the level of the sixth cervical vertebra from the third cervical vertebra of the neck. And it is located at the intersection of the flow of air and the flow of swallowed food.

There are two holes in the larynx where there are carvin gaps. This area is the vocal cords and glottis. The air that is expelled from the

lungs rises up along the trachea, hitting the underside of the vocal cords, and vocalizing is performed. The function of the larynx is as follows. First, protect the airway by closing the airway so that food can not be ingested when it is swallowed or vomited. Second, it vibrates to realize vocalization. Third, it is involved in respiration by narrowing at expiration and widening at inspiration. Fourth, close the larynx to fix the chest wall, breathing to raise the abdominal pressure is involved in the regulation of the chest.

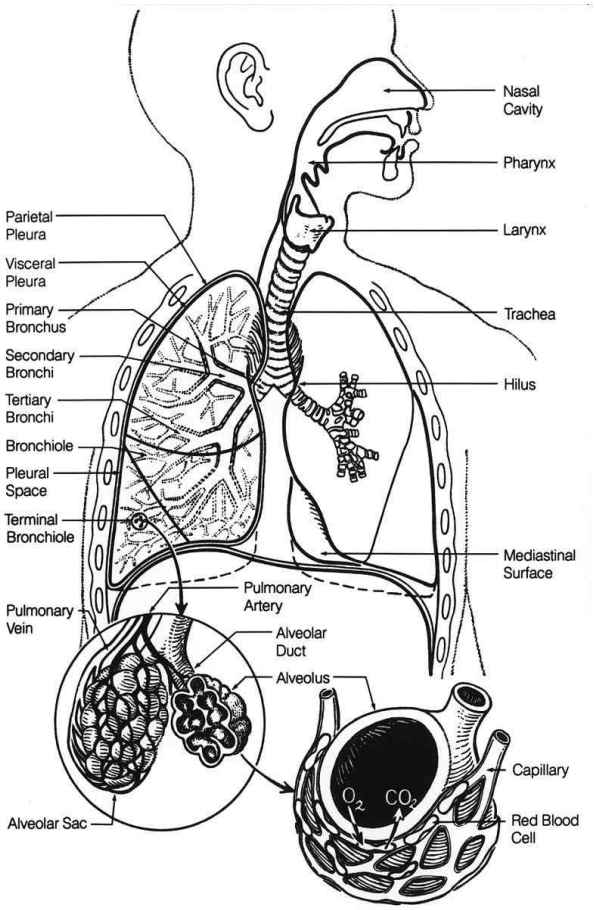

Figure 1. Respiratory system

This means a biological system responsible for gas exchange. The upper respiratory system consists of nose, nasal cavity, sinus, pharynx and larynx. The lower respiratory system consists of the lower larynx, trachea, bronchi, bronchioles, and alveoli

Source : "Respiratory System" , Last modified January 1, 2001, https://visualsonline.cancer.gov/details.cfm?imageid=1773, unknown illustrator, National Cancer Institute, Use after permission

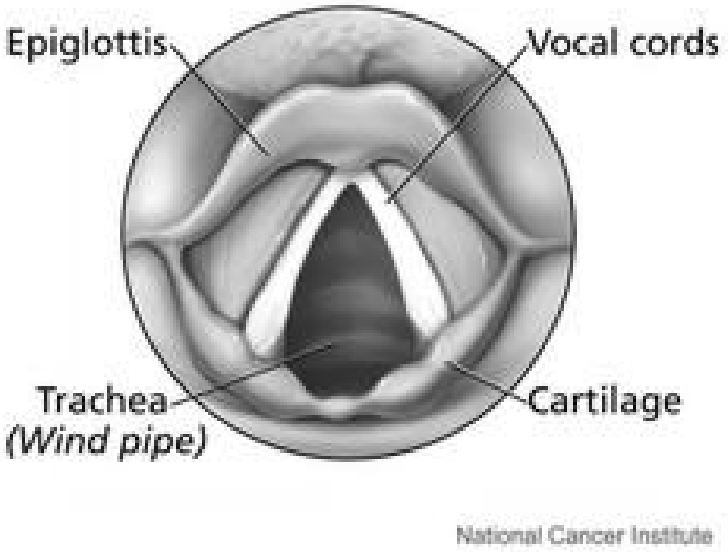

Figure 2. Larynx

The function of the larynx is as follows. First, protect the airway by closing the airway so that food can not be ingested when it is swallowed or vomited. Second, it vibrates to realize vocalization. Third, it is involved in respiration by narrowing at expiration and widening at inspiration. Fourth, close the larynx to fix the chest wall, breathing to raise the abdominal pressure is involved in the regulation of the chest.

Source : "Larynx" , Last modified September 20, 2007, https://visualsonline.cancer.gov/details.cfm?imageid=4370, alan hoofring, National Cancer Institute, Use after permission

1.2. Mechanical ventilator

The mechanical ventilator is a device that helps the respiration by inflating the alveoli by artificially inflating the air into and out of the lungs in patients who are physically unable to breathe or whose respiration is insufficient. It is important to set the ventilator appropriately according to the patient's condition, which greatly affects the outcome of the patient. The ventilator is divided into a negative pressure ventilation system and a positive pressure ventilation system.

The negative pressure ventilation system works by exposing the patient's chest surface to sub-atmospheric pressure [18]. The ventilator is a long, large tank that wraps around the patient's head. The patient's neck is sealed with a rubber gasket to keep the patient's head at atmospheric pressure and expose the patient's chest surface to sub-atmospheric pressure. When sub-atmospheric pressure is applied to the chest surface, the chest expands and the pressure in the pleura and alveoli decreases below atmospheric pressure, causing the air to travel from the airway to the alveoli and perform the inspiration. After this, when the pressure surrounding the chest is raised to atmospheric pressure, exspiration occurs passively due to the resilient recoil of the respiratory system. This is one of the first pressurizers for long-term ventilation.It was developed in 1929 and was widely used in polio cases that hit the world in the 1940s.

The positive pressure ventilation works by increasing the patient's airway pressure. Airway pressure is increased, causing air to flow through the airway, causing inspiration.. When the airway pressure is reduced to zero, breathing occurs due to the elasticity of the chest wall

and lungs. This system was designed to supply oxygen to fighter pilots flying at high altitudes during World War II. After that, as a safe endotracheal tube (e-tube) was developed, the positive pressure ventilation system replaced the negative pressure ventilation system. At the onset of polio in the 1950s, the device was used extensively in Scandinavia and the United States, resulting in a reduction in patient mortality.

Figure 3. Positive pressrue ventilation system

Source : “Newborn baby with hyperbilirubinemia on breathing machine or ventilator with pulse oximeter sensor and peripheral intravenous cath” , Final correction unknown, https://www.dreamstime.com/stock-photo-newborn-baby-hyperbilirubinemia-breathing-machine-ventilator-pulse-oximeter-sensor-peripheral-intravenous-cath-image91345414, Valentyna Lomova, Dreamstime, Use after permission

1.3. E-tube

Endotracheal intubation (EI) is an intubation of the e-tube made of plastic inside the trachea to ensure airway [figure 4]. This procedure allows efficient oxygen supply and carbon dioxide emissions. This is an essential procedure for patients with cardiovascular disease, cerebrovascular disease, multiple trauma, and severe pneumonia.

The speed and accuracy of this EI is very important because it is directly related to the patient's survival. However, the success of this procedure depends largely on the proficiency of the practitioner. Conventional EI allows the practitioner to visually check the trachea entrance through the oral cavity by tilting the patient's head back and intubating the laryngoscope. Then, while keeping a close eye on the entrance of the organ, hold the tip of the tube by hand and push it in. This method requires a high level of proficiency, which often fails even for emergency medical personnel trained for many years. In addition, there are many cases where the procedure fails because of the inability to obtain a visual acuity according to the individual disease and physical characteristics of the patient, such as a trauma patient requiring cervical fixation, a short neck, or obesity. Especially in the emergency rescue field, EI shows high failure rate. In an emergency situation such as cardiac arrest, the incidence of intubation was found to be 6 to 16% in the esophagus rather than in the trachea [16].

There are three major efforts to overcome these difficulties.

The first is the use of a video laryngoscope designed to provide a field of view within the laryngeal. The device is similar in shape to the laryngoscope. It is designed to acquire images of the laryngeal

lumen. Thus, the practitioner can intubate the tube while observing the airway entrance through the image seen on the external display. Video laryngoscope has advantages that is relatively easy to secure the vision and can be used in patients with fixed cervical vertebrae. However, it has a disadvantage of requiring a higher level of skill than the existing laryngoscope.

The second is the use of a bronchoscopy. The practitioner can observe the larynx through the bronchoscopy and watch the airway entrance. In addition, the direction of the endoscope can be manipulated as desired, and entry into the trachea is easy. Therefore, the e-tube can be pre-mounted on the device, the endoscope direction can be adjusted, and the intubation tube can be easily inserted.

Bronchoscopy also has advantages that is relatively easy to secure the vision and can be used in patients with fixed cervical vertebrae. The endoscope can also be manipulated to actively enter the tube within the trachea. However, as with video laryngoscopes, it requires a high degree of proficiency.

Figure 4. E-tube

Figure 5. EI

Source : "Anaesthesiologist performing intubation", Final correction unknown, https://www.dreamstime.com/stock-photography-anaesthesiologist-performing-intubation-image5194532, Andrei Malov, Dreamstime, Use after permission

1.4. Supraglottic airway (SGA)

The third is the use of a SGA [figure 5]. It is a device to support breathing on or around the vocal cords without passing through the vocal cords [24]. It is equipped with a specially designed cuff that covers the larynx in the laryngeal lumen. When the device is intubated, the operator pushes the tube to the end without having to observe the laryngeal lumen to check the larynx. After the infusion of air into the cuffs, the airway closes against or around the glottis to form a closed loop between the trachea and the mechanical ventilator. In this paper, we have studied the laryngeal mask airway (LMA), IGEL and combitube.

The LMA has an inflatable cuff of elastic material with a diameter of 52.9 mm larger than the inner diameter 20.2 mm of the laryngeal lumen around the supraglottis at the end [figure 5.a)]. After the end of the airway is inserted, the cuff is inflated and air pressure is applied to the laryngeal lumen. At this time, the laryngeal lumen expands and blocks the space between the laryngeal lumen and the cuff. This creates airtightness between the cuff and the supraglottis, creating an air line between the oxygenator and the trachea. Then, the pressure applied from the cuff to the lumenal lumen acts as a vertical drag to generate a frictional force. This maintains the initial position even when an external force is applied to the LMA.

The IGEL has an elastic non-inflatable cuff at the end with a diameter of 47.0 mm larger than the inner diameter 20.2 mm of the laryngeal lumen around the glottis [figure 5.b)]. Without any additional work, such as infusion of air at the cuff, the inflatable cuff pressurizes

the laryngeal lumen. At this time, the laryngeal lumen expands and blocks the space between the laryngeal lumen and the cuff. This creates airtightness between the cuff and the supraglottis, creating an air line between the oxygenator and the trachea. Then, the pressure applied from the cuff to the lumenal lumen acts as a vertical drag to generate a frictional force. This maintains the initial position even when an external force is applied to the IGEL.

The combitube has a distal cuff with a diameter 31.3 mm at the end and a proximal cuff with diameter 52.0 mm at the middle [figure 5.c)]. When the air is injected into the distal cuff, it is inflated and pressure is applied to the esophagus. The pressure expands the esophagus and blocks the empty space between the esophagus and the distal cuff. This provides sealing between the esophagus and the distal cuff. When the air is injected into the central cuff, it is inflated and pressure is applied to the laryngeal lumen. The pressure expands the laryngeal lumen and blocks the empty space between the laryngeal lumen and the central cuff. This provides sealing between the laryngeal lumen and the central cuff. The tube have twin lumen which the air moves. One lumen is connected to the hole located at the end of the tube and another lumen is connected to the four holes located at the middle of the tube. When the distal cuff is inserted into the trachea, the combitube transmits air through a lumen connected to the hole located at the end of the tube. When the distal cuff is inserted into the esophagus, the combitube transmits air through a lumen connected to four holes located at the middle of the tube. Through this, the esophagus located above the distal cuff, laryngeal lumen under the central cuff and trachea seal are formed to form an

oxygen-respiratory-airway line. In this way, the esophagus located above the distal cuff, laryngeal lumen under the central cuff and supraglottis seals are obtained. It forms a line between the oxygen respirator and the trachea. The pressure applied from the distal cuff to the esophagus and from the central cuff to the lumenal lumen acts as a vertical drag to create a frictional force. This allows the combitube to maintain its initial position even when an external force is applied to the tube.

a) b) c)

Figure 5. SGA a) LMA b) IGEL c) combitube

1.5. Research Needs: Problems of SGA

Supraglottic airway has the advantage that the required skill level is relatively low. Therefore, it is widely used as an alternative to EI in the field of medical practice [12]. However, in recent large-scale studies of cardiac arrest patients, the results of spontaneous circulation recovery, survival rate, and neurological prognosis are reported to be worse than those obtained with EI when using a SGA [13, 15, 16]. In addition, in preclinical studies using the cardiac arrest model of pigs, it has been reported that carotid blood flow and pressure decreased during CPR [9, 10, 11]. The above phenomenon is presumed to be caused by pressing the carotid artery with the pressure applied to the laryngeal lumen by the cuff [6, 7, 12, 37]. In the above-mentioned large-scale study, the prognosis of the patient using the SGA was bad and the above effect is presumed to be the cause. However, a clear basis for this has yet to be proven.

1.6. Research objective

The purpose of this study is as follows. First. identify the problems that arise in terms of hemodynamic aspects, especially brain survival, during EI. Second, analyze the causes of the problem. Third, develop the new-SGA to solve the problem.

In order to identify the problems in the carotid artery flow during supraglottic airway intubation (SI), preclinical studies are carried out on three kind of SGAs (LMA, IGEL, combitube) and e-tube by using 12 pigs heart arrest model. In this study, we compare the data during SI

with the data during EI and identify the problems of SGA. In order to analyze the cause of the problems during SI, three types of SGA and e-tube were implanted to pig and computed tomographic images are taken. After making the 3D model of pre- and post-intubation SGA, carotid artery, laryngeal lumen by using the photographed images, we conduct the appearance analysis. Among these, 3D model of pre-intubation laryngeal lumen and post-intubation SGAs are output to 3D printer for more detailed appearance analysis. Finally, we develop new-SGA to develop a new airway maintenance method which is most advantageous in terms of brain survival in cardiac arrest patients. To develop new-SGA, the first principle is to mechanically analyze the fixing principle of existing-SGA and the principle that the carotid artery is pressurized by the cuff to make hemodynamic difference. Secondly, the mechanistic viewpoints of the new-SGA that improve carotid artery blood flow and blood pressure decrease by reducing carotid artery pressure while maintaining airtightness are presented. Thirdly, the new-SGAs are produced, and conduct in vitro and in vivo performance evaluation.

Chapter 2. Method

2.1. Measurement of the effects of the existing-SGA on carotid artery blood flow using animal models

We conducted preclinical studies in order to identify the problems of the SGA by comparing the data from the SI with the data from the EI. The preclinical study consisted of six experimental groups according to the order of intubation of each SGAs, and two pigs were assigned to each experimental group. Randomization was carried out to cross-test for each SGAs [figure 7]. The major data in this study are carotid arterial blood flow (mL/sec) and carotid arterial blood pressure (mmHg). After inducing cardiac arrest in the pigs, SGAs and e-tube were alternately intubated and the data was measured [figure 8]. The data measured in each SI section were averaged together with the data measured in the The EI section, which is the base section. Considering the difference between each pig, data of the EI as a baseline was used as a denominator and the change in data of the SI was calculated as a percentage (%).

	SGA#1	SGA#2	SGA#3
Group#1(two pigs)	LMA	IGEL	Combitube
Group#2(two pigs)	LMA	Combitube	IGEL
Group#3(two pigs)	IGEL	Combitube	LMA
Group#4(two pigs)	IGEL	LMA	Combitube
Group#5(two pigs)	Combitube	IGEL	LMA
Group#6(two pigs)	Combitube	LMA	IGEL

Figure 7. Classification of experimental group according to order of airway intubation

The preclinical study consisted of six experimental groups according to the order of intubation of each SGAs, and two pigs were assigned to each experimental group. Randomization was carried out to cross-test for each SGAs

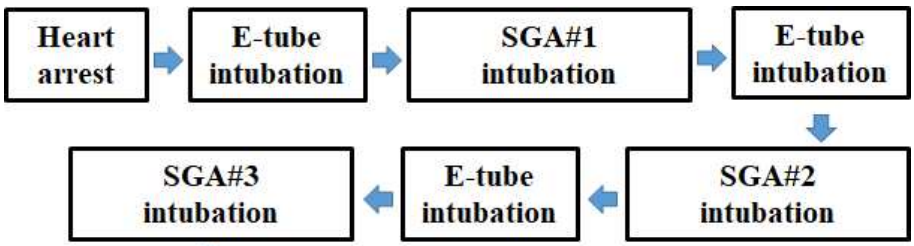

Figure 8. Preclinical research stage.

After inducing cardiac arrest in the pigs, SGAs and e-tube were alternately intubated to compare and analyze the data during EI and SI

Figure 9. SI in preclinical studies,

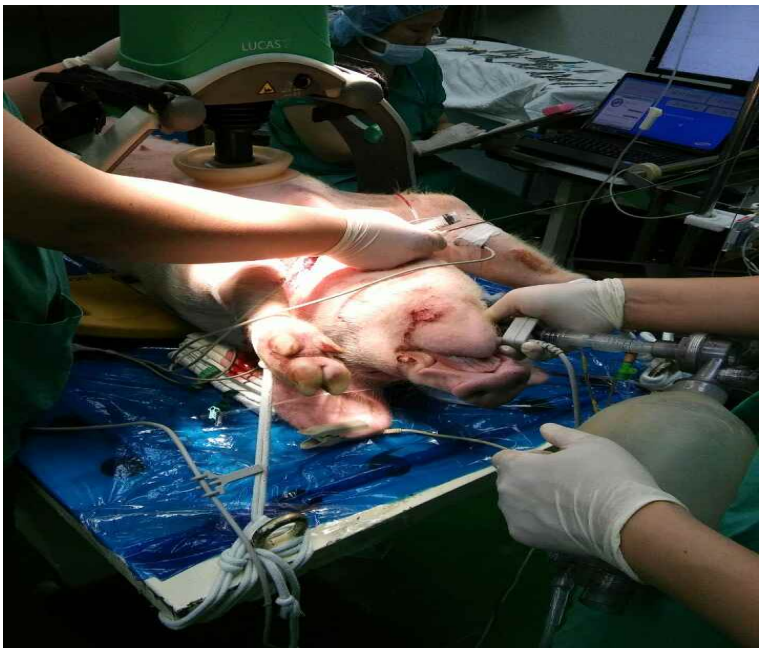

Figure 10. Mechanical chest compression CPR in preclinical studies

2.2. Analysis of blood vessel shape using computed tomography image

Computed tomography images are continuous images taken with a fan-shaped x-ray with a width of 1-20 mm, moving the patient using an electric table. This represents three-dimensional information of the patient's body and organs [8, 9]. The image is composed of pixels [10], and has a gray scale, which is a stepwise division of brightness from white to black. Using these images, image processing is possible such as converting the horizontal plane into the coronal plane and the sagittal plane, image flattening, image boundary enhancement, grayscale adjustment, and 3D modeling etc [11].

In order to analyze the cause of the problem of the SGA confirmed in the preclinical experiment, the pigs were alternately intubated with e-tube and three SGAs(LMA, IGEL, combitube) and taken CT images. Using the above images and Seg3D and Meshmixer, 3D models of SGAs, carotid artery and laryngeal lumen before and after intubation were prepared and then analyzed for appearance. The 3D model of the laryngeal lumen of pig before intubation and SGAs after intubation were output to FDM 3D printer (3DP-110F (Single), HYVISION, Gyeonggi-do, Korea).

2.2.1. Computed tomography

Two pigs were intubated with e-tube and three types of SGA and

the computerized tomography was performed [figure 11]. A computerized tomography of the SGA before the intubation was also performed. Then, a 3D model of the SGA was made. This is compared with the 3D model of the SGA after the intubation. In accordance with the IACUC standard operating guidelines, pigs were injected with one of the Zoletil vials used as animal anesthetics in an animal laboratory and then inhaled with isoflurane [38]. When moving from an animal testing laboratory to a computerized tomography site, intravenous anesthesia was continuously injected so that pigs did not feel pain in accordance with pre-clinical research ethics standards and regulations. After arriving at the computerized tomography site, the pig's back was laid down on the floor and simulated a posture similar to that of a person who used a real airway. The pigs were held horizontally constant to eliminate interference from other elements [17].

The images were taken using a Lightspeed Ultra 8 CT Scanner (GE, Boston, USA) by 1.25 mm intervals. The internal carotid artery was visualized by injecting contrast agent. In this study, the most deeply trained airway is e-tube that is intubated with trachea or combitube that is intubated with esophagus. In order to acquire images of all sections of the carotid artery affected by the airway, the carotid artery located at the lower side was selected and injected with contrast agent. The contrast agent spreads in the blood, and the position and concentration of the contrast agent changes over time [figure 12]. The time that contrast agent is well propagated to the region of interest and has the optimal concentration for image analysis was set (1 minute 25 seconds) The images were taken at the same time after contrast agent injection for all airway.

Figure 11. Computed Tomography

a) b)

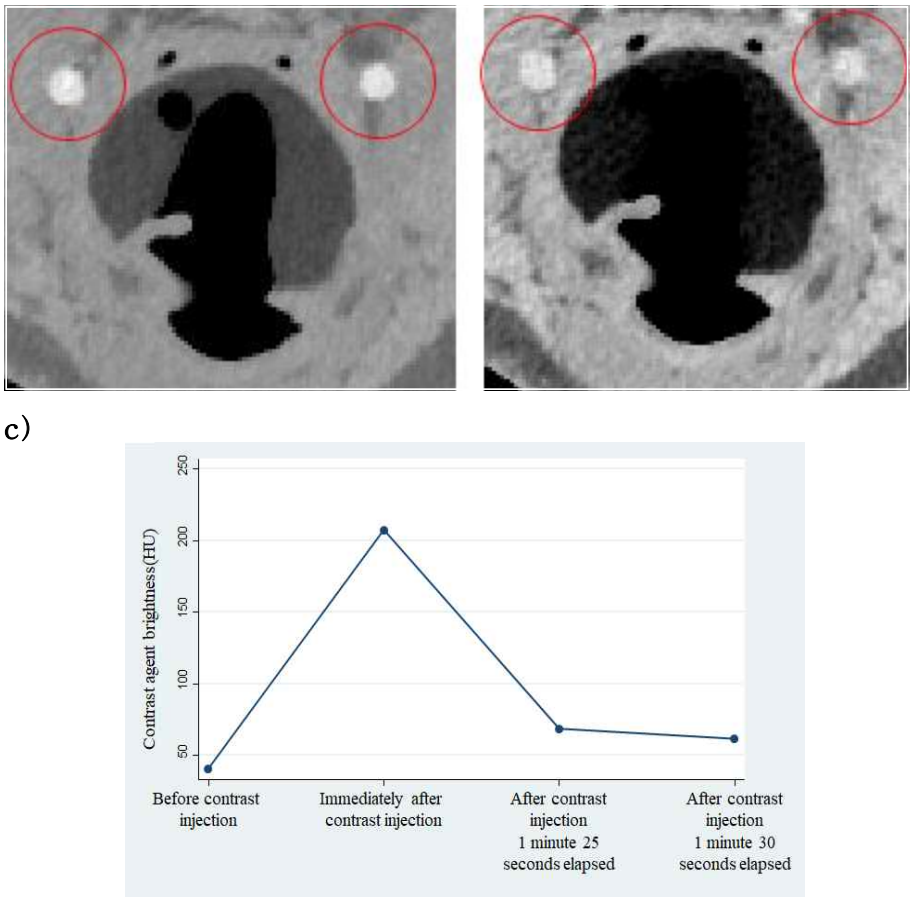

Figure 12. Brightness change with time after contrast injection

a) Computed tomography of the carotid artery at 1 minute and 25 seconds b) Computed tomography of the carotid artery at 1 minute and 30 seconds c) Contrast photograms over time after contrast injection. The contrast agent spreads in the blood, and the position and concentration of the contrast agent changes over time. The time that contrast agent is well propagated to the region of interest and has the optimal concentration for image analysis was set (1 minute 25 seconds)

2.2.2. Analysis of vessel shape using 3D model

Through the analysis of the appearance, we analyze the effect of the SGA on the living body. For this, 3D models of Laryngeal lumen, airway and carotid artery before and after intubation were made using Seg3D and Meshmixer. The 3D modeling consists of the following three steps [figure 13, 14] [19]. The first step is to cut out the region of interest in the CT image. In the second step, the separated CT images are filtered and segmented. In the third step, a 3D model is constructed with segmented CT images and post-processed.

In the first step, the analysis area within the CT image is cropped [figure 15]. Cropping can crop one or more layers to a specified size on the axial, coronal, and sagittal planes. This limits the analysis area and removes the rest to facilitate facade analysis. This facilitates the appearance analysis. Also, by reducing the amount of analytical data, the research efficiency is improved by shortening the data processing time.

In the second step, the separated CT images are filtered and segmented [figure 16, 17, 18]. Filtering reduces noise in the image. Segmentation extract the necessary part according to the light and darkness in the image The median filter was applied to the filtering. The median filter is a nonlinear filter that reduces noise. This finds an intermediate value between adjacent pixels and replaces the original pixel. This applies to all pixels other than the edge portion. The formula for the median filter is:

$$I_{new}(x,y) = \sum_{j=-1}^{1}\sum_{i=-1}^{1} 1 \times I_{old}(x+i, y+i) \quad (1)$$

$$I_{new,\ normalizezd}(x,y) = \frac{1}{\sum_{j=-1}^{1}\sum_{i=-1}^{1} 1} \sum_{j=-1}^{1}\sum_{i=-1}^{1} 1 \times I_{old}(x+i, y+i) \quad (2)$$

In the above formula, x, y are coordinate values of a pixel and I is a pixel value. The segmentation is a function of dividing the data having the lightness and darkness within the specified range. This is an essential step in 3D modeling.This is done using the threshold function. It is one of the most basic semi-automatic tools used in Seg3D. This can be set in two ways. The first is to set the maximum and minimum values of the boundary value through the slider provided in the tool window. The second is to set seed points in the CT image and change the boundary value to include the illumination value of points. However, it is necessary to edit the noise region which has the similar illumination value to the region of interest. To do this, we manually removed the noise region using the paintbrush and polyline function.

In the third step, 3D models are implemented with segmented CT images and post-processed [figure 19, 20]. The 3D model is implemented by stacking segmented areas. This was done using Seg3D's isosurface compute function. Postprocessing is operation to remove the noise of the 3D model and smooth the surface for appearance analysis. This was done by using the smooth function of the Meshmixer.

The preoperative 3d models of laryngeal lumen before intubation and

SGAs after intubation were output by FDM 3D printer [figure 21, 22]. This led to a more detailed appearance analysis

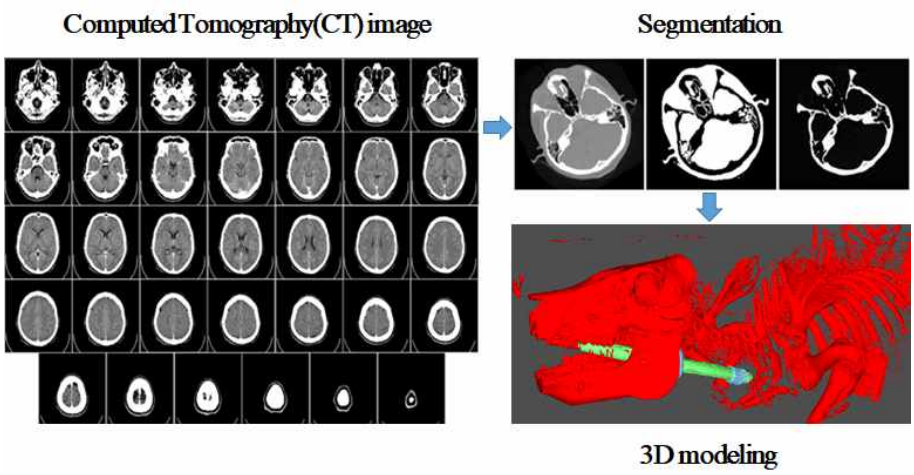

Figure 13. 3D modeling process

The 3D modeling consists of the following three steps. The first step is to cut out the region of interest in the CT image. In the second step, the separated CT images are filtered and segmented. In the third step, a 3D model is constructed with divided CT images and post-processed.

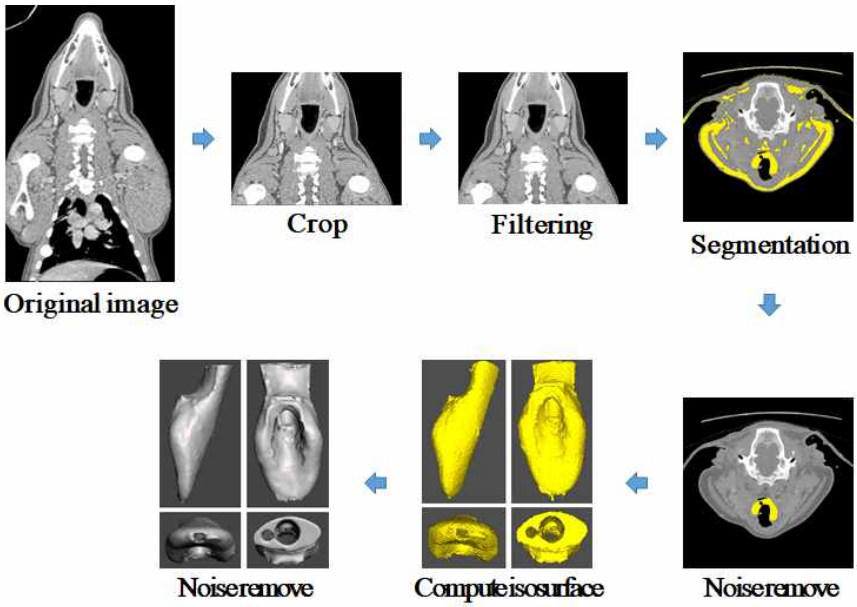

Figure 14. 3D modeling process by Seg3D

a) b)

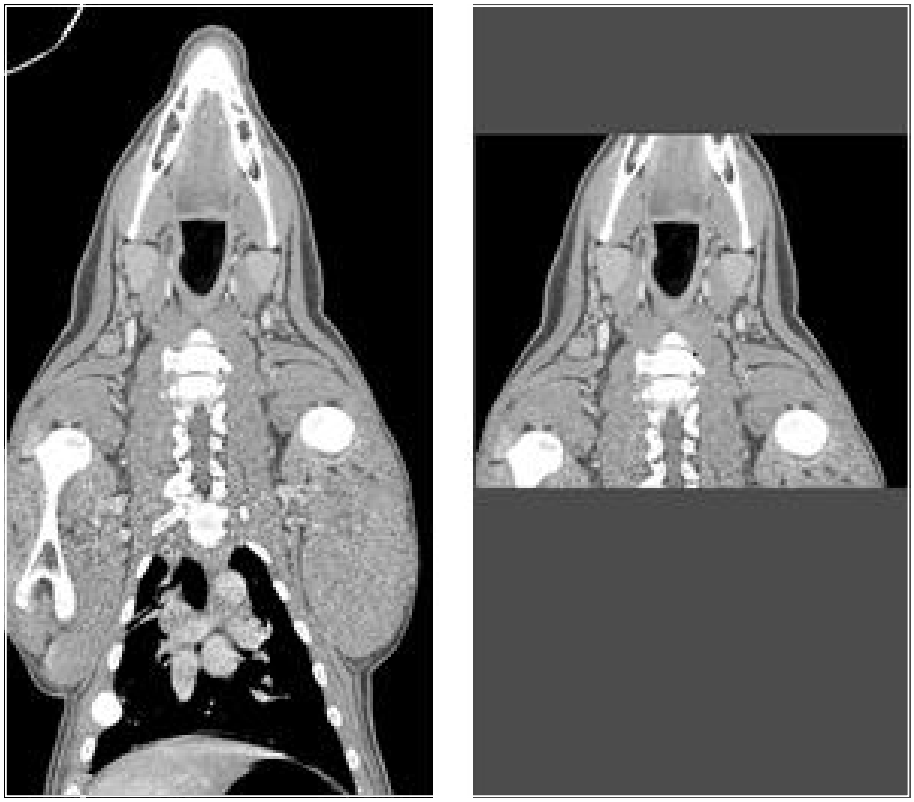

Figure 15. Cropping a) before b) after

a)

b)

Figure 16. Filtering a) before b) after

a)

b)

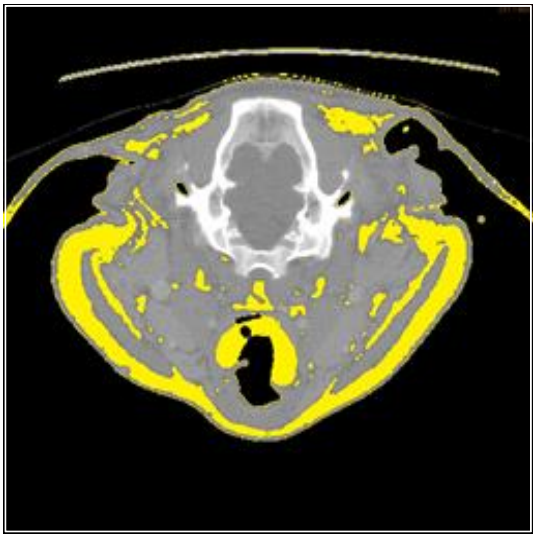

Figure 17. Segmentation a) before b) after

a)

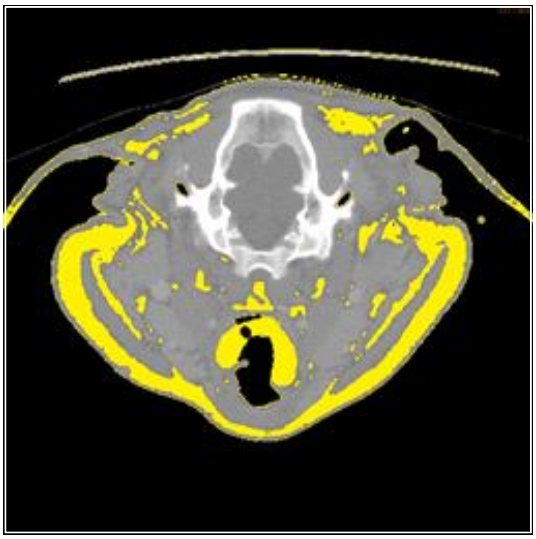

b)

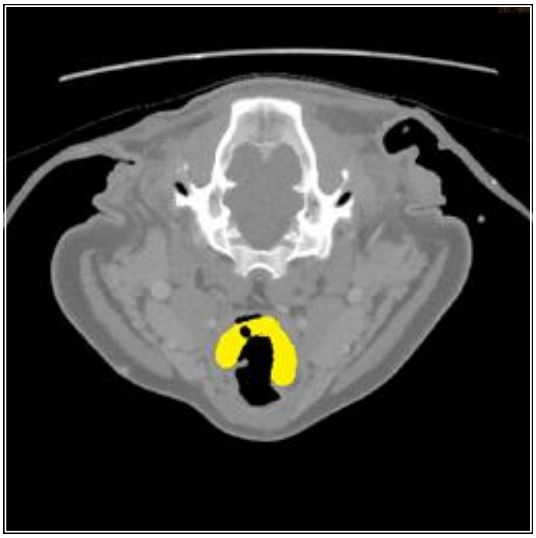

Figure 18. Paintbrush and polyline function a) before b) after

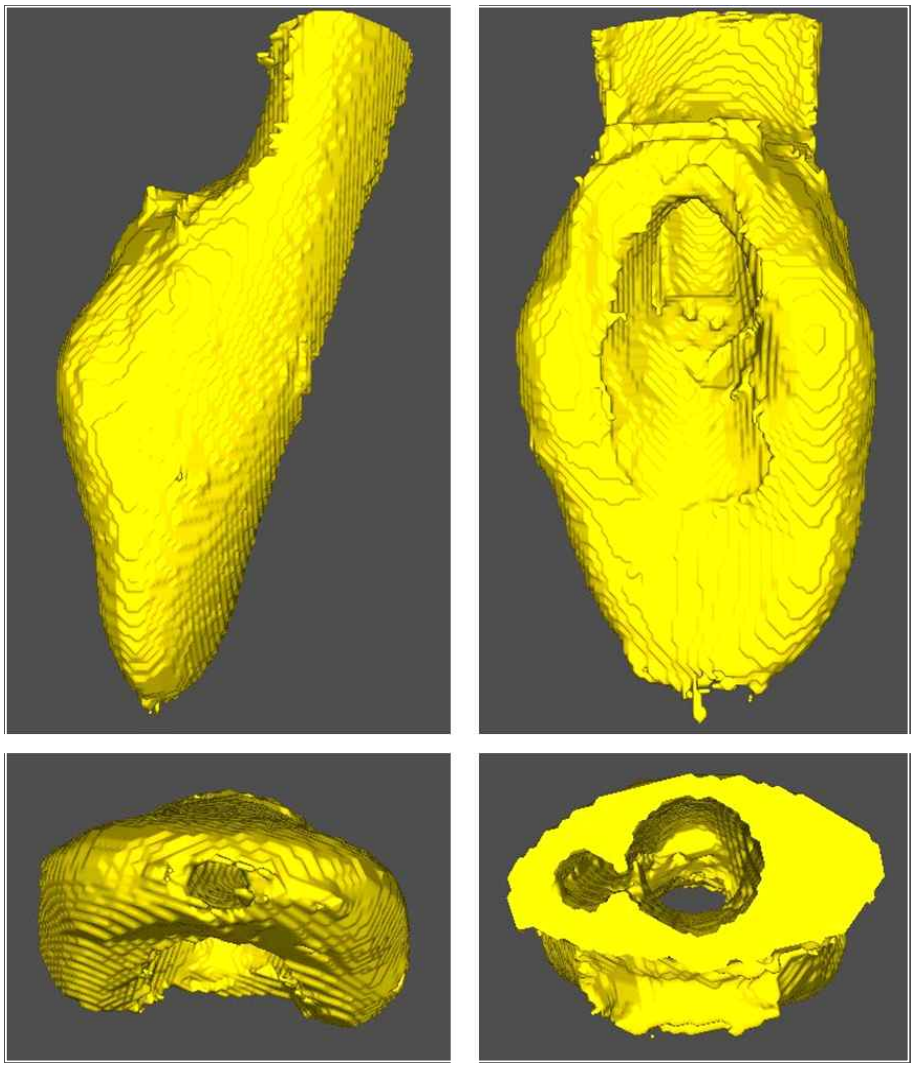

Figure 19. 3D models implementation

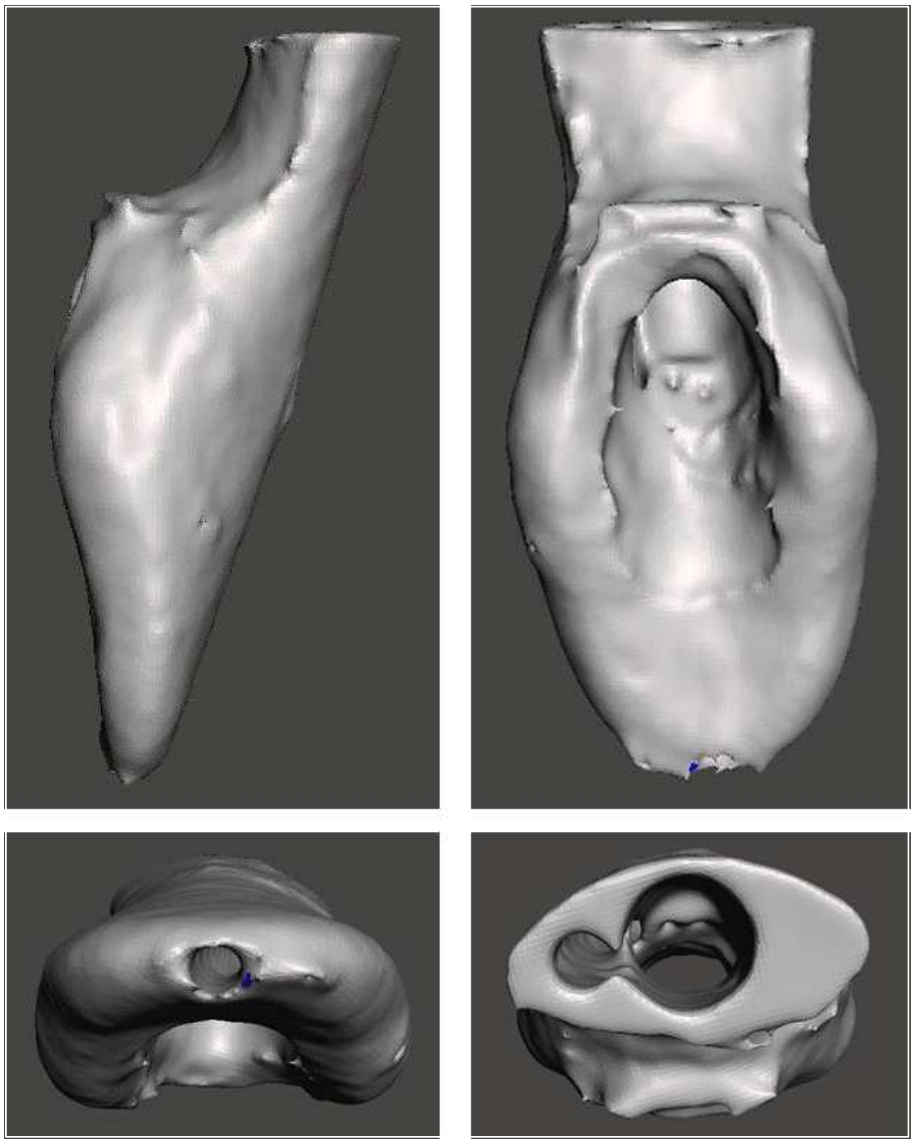

Figure 20. Post-processing

a)

b)

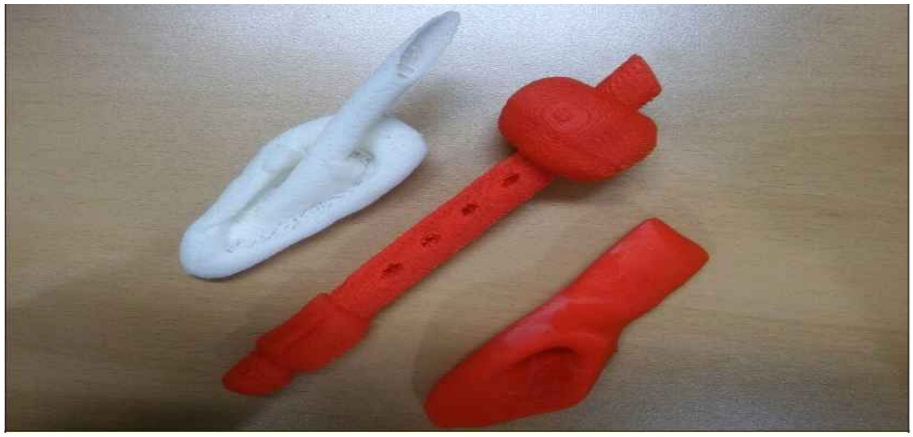

Figure 21. Output of FDM 3D printer a) laryngeal lumen before intubation b) SGAs after intubation : LMA (left), combitube(middle), IGEL(right)

2.3. Design and manufacture of new-SGA

We make new-SGAs in order to solve the problem of the existing-SGAs. The sealing and fixing principles of LMA and IGEL are similar. Therefore, new-SGAs are fabricated for two types of SGAs, IGEL and combitube without LMA. The process of manufacturing new-SGAs is as follows. For the first time, we analyze SGAs mechanically. The second new-SGAs are presented and the principle is analyzed mechanically. The third new-SGAs are made. Fourth, the performance of new-SGAs is evaluated in vitro and in vivo.

2.3.1. Mechanical analysis of the existing-SGAs

In order to remedy the problems of the existing-SGAs, mechanical analysis is needed. First we analyze the principle of the sealing between the trachea and the ventilator. Second we analyze the principle of fixing to the laryngeal lumen. Third The principle of reducing the blood flow and blood pressure of the carotid artery by the pressure applied by the cuff to the laryngeal lumen was analyzed.

2.3.1.1. Mechanical analysis of the sealing of existing-SGAs

The existing-SGAs implements trachea and mechanical ventilator seals through a cuff having a diameter longer than the inner diameter of the laryngeal lumen. The maximum diameter of the LMA / IGEL / combitube proximal cuff is 52.9 / 47 / 52.9 mm. Existing-SGAs all have diameters greater than the maximum inner diameter of the laryngeal lumen 20.2 mm. Because the diameter of the cuff is longer

than the inner diameter of the laryngeal lumen, the cuff pressurizes the laryngeal lumen during intubation. The laryngeal lumen expands according to the shape of the cuff by this pressure. And closing the laryngeal lumen by blocking the space between the laryngeal lumen and the glenohumeral ceramic cuff. The LMA and IGEL cover the larynx with the cuffs to close the laryngeal lumen. This leads directly to the larynx and SGAs. Thus, creating a closed loop between the trachea and the mechanical ventilator. The combitube closes the laryngeal lumen with a proximal cuff. The esophagus is closed with a distal cuff. This provides a closed loop between the trachea, lower laryngeal lumen, upper esophagus, and mechanical ventilator.

2.3.1.2. Mechanical analysis of the fixing of existing-SGAs

The existing-SGAs is fixed by the frictional force generated between the cuff and the laryngeal lumen. The diameter of cuff is longer than the internal diameter of the laryngeal lumen. In this case, the cuff pressures the laryngeal lumen during intubation. The pressure acts as a vertical drag to generate frictional force between the cuff and the laryngeal lumen. It maintains its position even when an external force is applied to SGAs. The above principle can be explained by the following equation.

$$f_k = \mu_k N \tag{3}$$

In the above formula, $f_k$is kinetic frictional force (N), μ_k is kinetic friction coefficient, N is vertical drag force (N).

2.3.1.3. Mechanical analysis of carotid blood flow and pressure reduction by existing-SGAs

In the previous study, it was confirmed that the carotid artery was compressed due to pressure applied by the cuff to the laryngeal lumen by intubation of SGAs through analysis of the CT images. The decrease in carotid artery blood flow and pressure due to decrease in cross-sectional area and increase in blood vessel length during carotid artery compression can be explained through the Darcy-Weisbach law. The Darcy-Weisbach law is a method of calculating the energy loss due to fluid motion in a closed conduit [28, 29, 30, 31]. The above equation can be used to analyze the capacity, diameter, and degree of pressure drop of the conduit. This is a necessary formula for analyzing fluid flow from one point to another. The Darcy-Weisbach law is derived from the energy equation of the bernoulli principle. The energy equation of the bernoulli principle is used to quantify the friction applied to the fluid between two points of the conduit as follows :

$$h_f = (\frac{V_1^2}{2g} + \frac{p_1}{\rho g} + z_1) - (\frac{V_2^2}{2g} + \frac{p_2}{\rho g} + z_2) \quad (4)$$

In the above formula, h_f is the energy loss due to the friction applied to the fluid that converted to the height of the fluid column (m), V is mean flow rate (m/s), g is the gravitational acceleration (m/s^2), p is the fluid pressure(pa), ρ is the fluid density (kg/m^3), z is the height of conduit (m). The Darby-Weisbach law derived from the above formula is as

follows.

$$h_f = \frac{fL}{D}\frac{V^2}{2g} \tag{5}$$

In the above formula, h_f is the energy loss (m), f is kinetic frictional forc e(N), L is length (m), D is diameter (m), v is flow rate (m/s). The coefficient of friction f is as follows.

$$f = \alpha + \frac{\beta}{\sqrt{V}} \tag{6}$$

In the above formula, α, β are coefficient determined by the diameter and material of the conduit, V is mean flow rate (m/s).

The Darcy-Weisbach law shows that the head loss is proportional to the length of the conduit and inversely proportional to the cross-sectional area. The existing-SGA cuff pressurize the laryngeal lumen during intubation. The pressure compresses the carotid artery to reduce the cross-sectional area and bend to increase the length. When analyzed by the Darwish-Weisbach law, it can be interpreted that the head loss is increased. As the head loss increases, vascular resistance increases. As the vascular resistance increases, the friction applied to the fluid increases. As the friction applied to the fluid increases, the energy loss increase. Finally, as the energy loss is increased, the carotid artery blood flow and blood pressure decreases.

The reduction of the carotid artery blood flow due to the decrease of the cross-sectional area due to compression of the carotid artery and the

increase of the blood vessel length due to the bow can be explained by the Hagen-Poiseuille's law [32, 33, 34, 35, 36]. The following formula explains the change in blood flow according to the cross-sectional area and the length of the blood vessel.

$$Q = \frac{K'' D^4 \Delta P}{l} \tag{7}$$

α, β are coefficient determined by the diameter and material of the conduit, V is mean flow rate (m/s).

In the above formula, Q is flow volume (m^3/s), K'' is coefficient, D is diameter (m), ΔP is pressure difference (pa), l is length (m). Of these, coefficient K'' is as follows :

$$K'' = 1836.7(1 + 0.033679\,T + 0.00022099\,T^2) \tag{8}$$

In the above formula, T is temperature (℃). The Hagen-Poisshou law derived from the above formula is below.

$$Q = \frac{\pi R^4 \Delta P}{8\mu l} \tag{9}$$

In the above formula, Q is flow volume (m^3/s), R is radius (m), ΔP is pressure difference (pa), μ is coefficient of friction, l is length (m).

The Hagen-Poisshou law shows that the flow volume is inversely proportional to the length of the conduit and proportional to the square of the radius. The existing-SGA cuff pressurize the laryngeal lumen

during intubation. The pressure compresses the carotid artery to reduce the cross-sectional area and bend to increase the length. When analyzed by the Hagen-Poisshou law, it can be interpreted that the flow volume is decreased.

2.3.2. Present the new-SGA

In the previous section, the principle of sealing, fixation and reduction of blood flow and pressure of carotid artery were analyzed mechanically. The pressure applied by the cuff to the laryngeal lumen increase the energy loss and reduces the carotid artery blood flow and pressure. In order to solve the above problem, new-SGAs satisfying the following conditions is required. First maintain air sealing to prevent air leakage. Second maintain frictional force between the cuff and the laryngeal lumen to fix its position even when an external force is applied to SGAs. Third reduce pressure applied by the cuff to the laryngeal lumen.

New-SGAs are designed with reference to US5957136, US4867149, US5249309 and US4936411 patents on ear plugs [figure 22] [25, 26, 27, 28]. These patents have been developed to overcome the problems encountered in conventional column ear plugs. Problems that occur in the ear plugs are as follows. First excessive pressure is applied to the eardrum wall. The wearer who feels discomfort tends to reduce the excessive pressure applied to the ear by pulling the ear plug from the ear canal to the outside. As a result, the sealing between the ear plug and the ear canal is not properly implemented, reducing the hearing protection function for wearing the earplug. The second problem is the

anatomical diversity. The individual earbud sizes of the users are different from each other. Therefore, the ear pillar must be manufactured in various sizes. This greatly increases cost and complexity in production. Furthermore, it is difficult for the user to wear ear plugs according to the size of the ear canal of his / her own.

To overcome these problems, the patents propose a multi-flange earplug with a plurality of thin plugs. Multi-flange earplug provide the following effects through the bending of thin plugs. First, it implements sealing between earplugs and ear canals. Second, it reduces the pressure on the ear canal. Third, it reduces the diversity of earplug size. When the ear plug is inserted into the ear canal, pressure is applied to the thin plug. The pressure causes the thin plug to bend to fit the shape of the ear canal. A curved, thin plug closes the gap between the ear canal and the plug to create sealing. The pressure applied to the ear canal is reduced to improve the discomfort of the wearer. The diameter is automatically adjusted to suit various ear canal sizes. This reduces the diversity of earplug size. It reduce manufacturing cost and complexity in production. It improves discomfort and difficulties by reducing user consideration when choosing earplugs.

The new-SGAs developed by applying the multi-flange shape [figure 23]. Thin plugs provide sealing by bending to fit the shape of the laryngeal lumen. And reduces the pressure on the laryngeal lumen to prevent blood flow and pressure reduction due to carotid artery compression. However, the vertical drag decreases when the pressure applied to the laryngeal lumen decreases. When the vertical drag decreases, the frictional force decreases and it is difficult to fix the new-SGAs. Generally, the frictional force of an object of the same

weight is constant regardless of its contact area. However, if the contact surface is sufficiently wet or oil film, the frictional force is proportional to the area [39]. The laryngeal lumen surface is mucous, so the frictional force in the laryngeal lumen is proportional to the contact area. The bending of the thin plug increases the contact area between the laryngeal lumen and the plug to maintain the frictional force. Therefore, it is possible to maintain the frictional force by increasing the contact area while reducing the pressure applied to the luminal lumen.

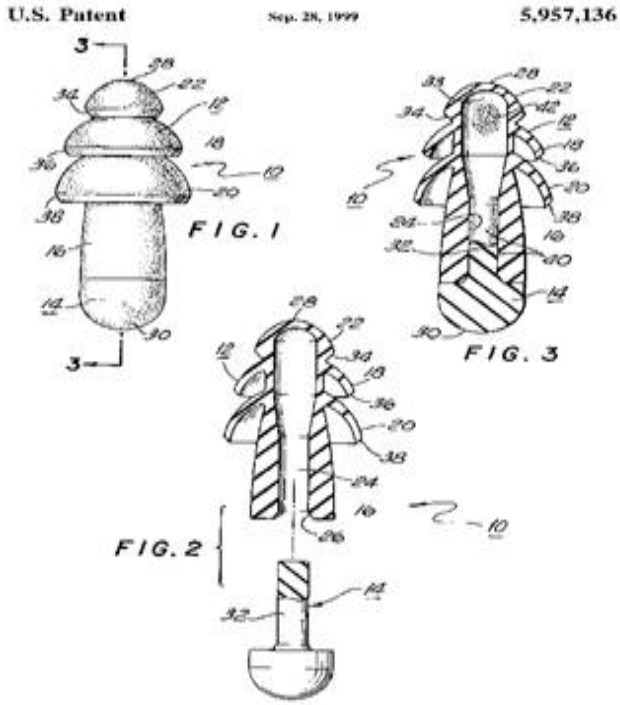

Figure 22. Multi-flange earplug

a)

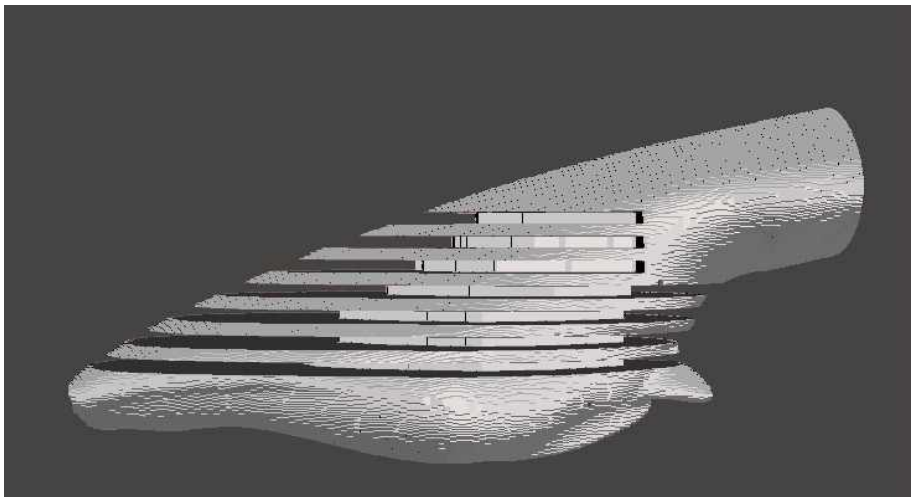

b)

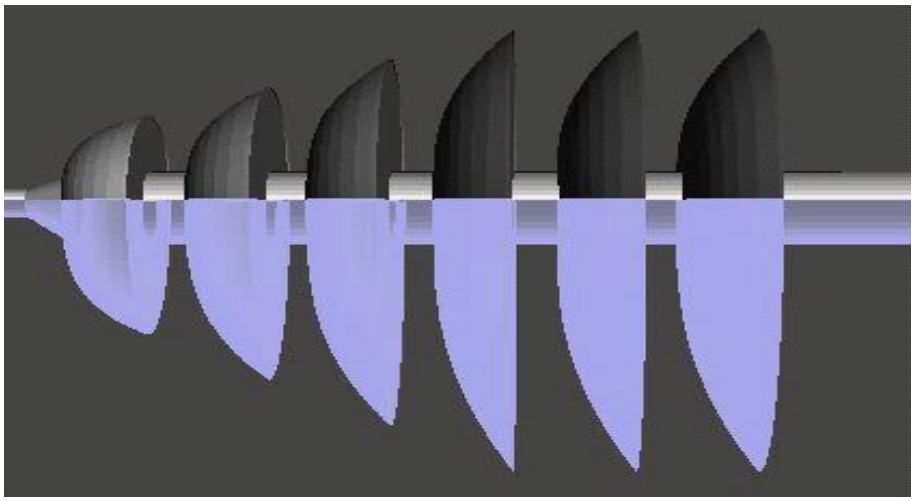

Figure 23. New-SGAs applying the multi-flange shape
a) new-IGEL b) new-combitube

2.3.3. Development of new-SGAs

The sealing and fixing principle of LMA and IGEL has similar. Therefore, we developed new-SGAs about IGEL and combitube except for the LMA. The development process of new-SGAs is like the figure 24. The material of new-SGAs cuff was selected as silicon which is similar in material to rubber used in the existing-SGAs cuff and has low toxicity and low cost of materials. Therefore, 3D models of new-SGAs were constructed using Seg3D and Inventor (Professional 2016, Autodesk Inc., California, USA) [figure 25]. And 3D models of mold for casting silicon were designed using Meshmixer and Inventor [figure 26]. The molds were produced by FDM 3D printer [figure 27]. We fabricated the cuffs of new-SGAs by casting silicon on the mold [figure 28] [20, 21, 22, 23]. The new-SGAs were fabricated by inserting and fixing the cuffs on the e-tube [figure 29].

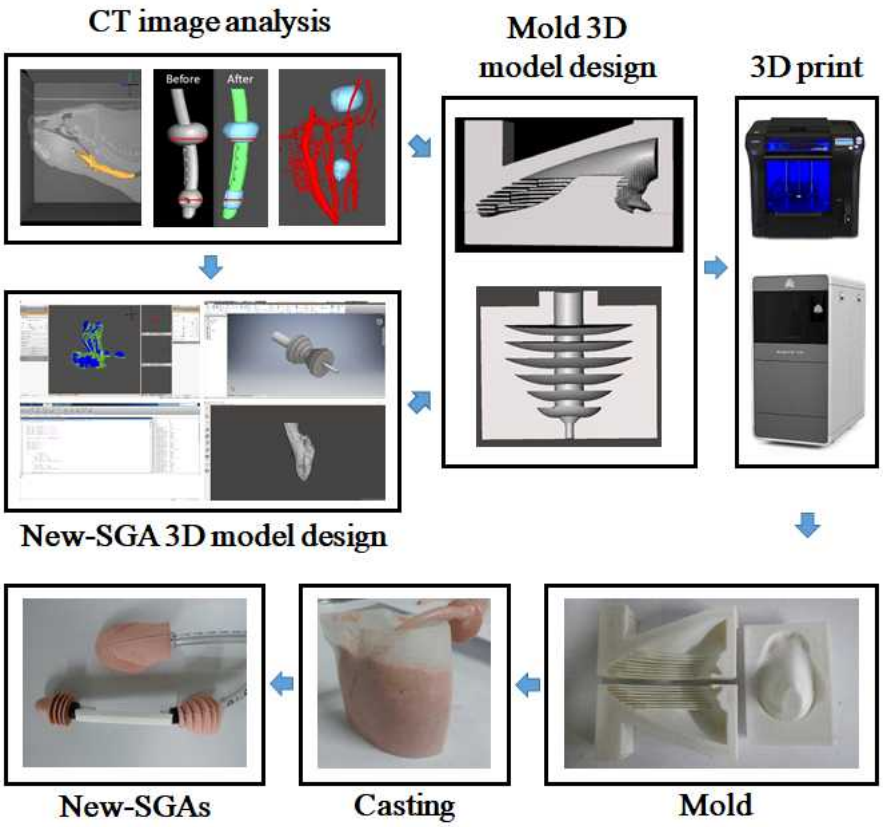

Figure 24. the development process of new-SGAs

a)

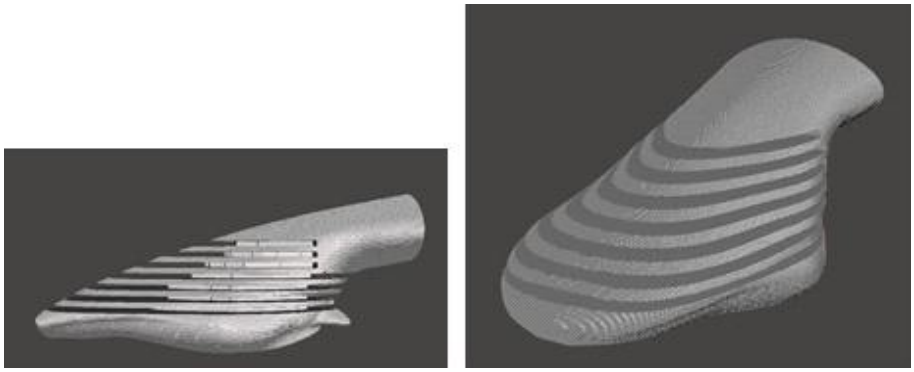

b)

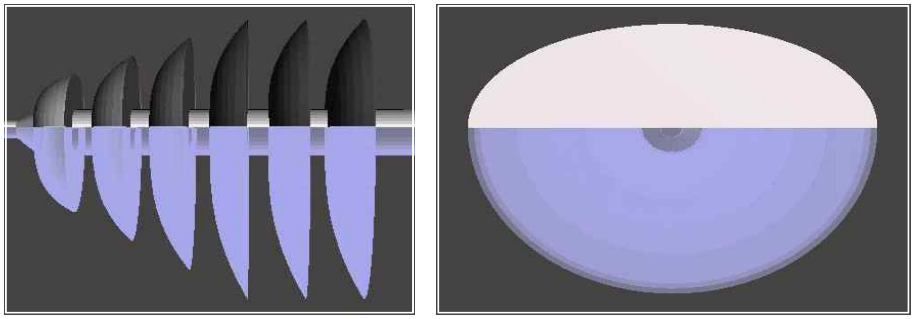

Figure 25. 3D models of new-SGAs a) new-LMA b) new-combitube

a)

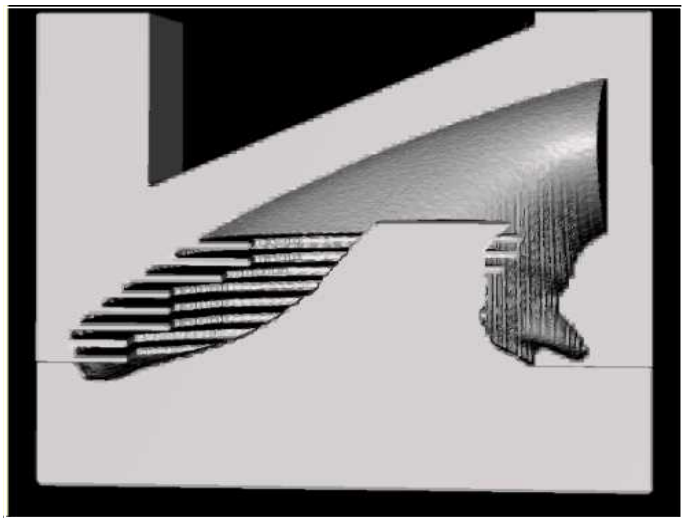

b)

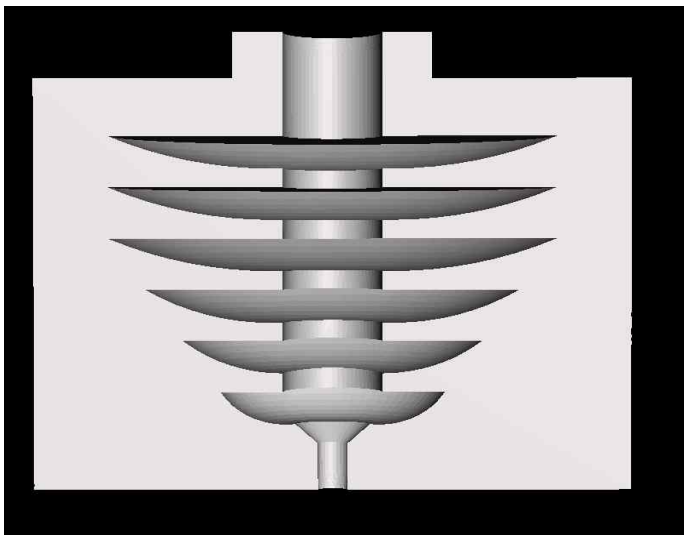

Figure 26. 3D models of mold a) new-LMA b) new-combitube

a)

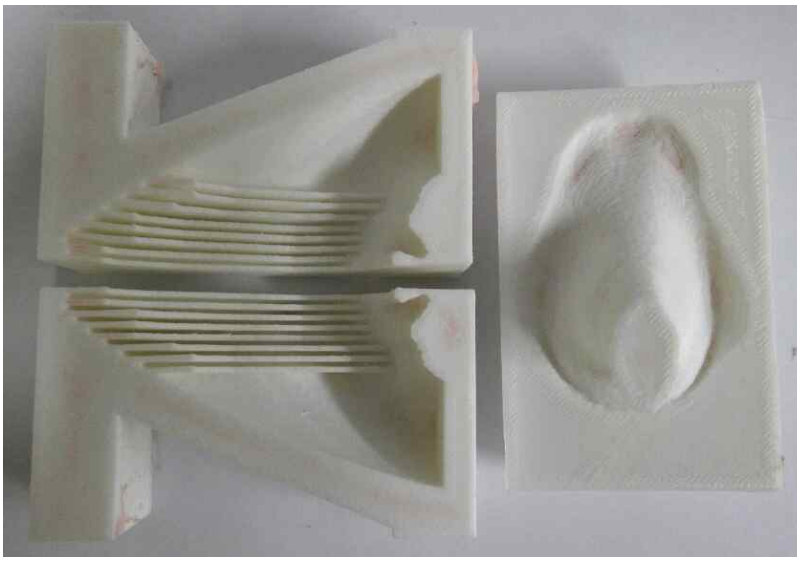

b) c)

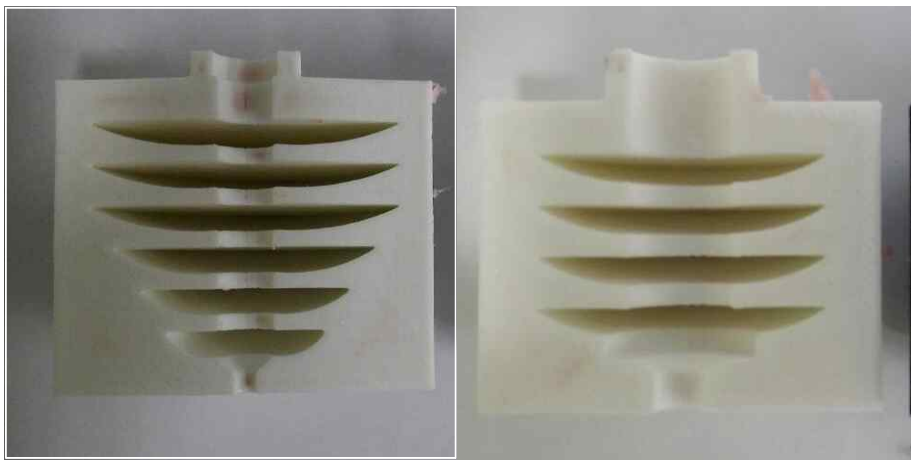

Figure 27. molds produced by FDM 3D printer
a) mold of new-IGEL b) mold of new-combitube proximal cuff
c) mold of new-combitube distal cuff

a)

b)

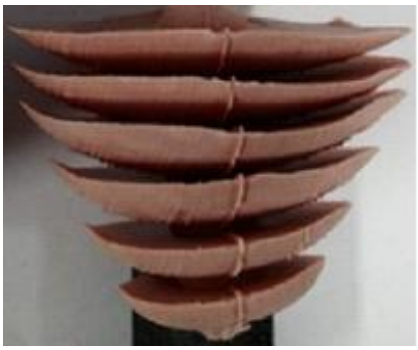

c)

Figure 28. cuffs of new-SGAs a) new-IGEL cuff b) new-combitube proximal cuff c) mold of new-combitube distal cuff

Figure 29. new-IGEL(left) new-combitube (right)

2.4. In-vitro performance evaluation of new-SGAs

In vitro experiments were conducted to verify the performance of the new-SGAs. First, the sealing performance of the new-SGAs was verified with a Airway maintenance mannequin. Second, the pressure applied by existing-, new-SGAs to the laryngeal lumen was measured and compared.

2.4.1. In-vitro performance evaluation about sealing

Airway maintenance mannequins, shape and material are similar to real human respiratory system, were checked for air leakage. The sealing performance of new-SGAs were verified by using the mannequin [figure 30]. Inside the mannequin, Sonogel (Parker Laboratories, Fairfield, USA) was applied to achieve a similar viscosity to the surface of the actual respiratory system. The open end of the mannequin was closed with a stopper to create close system in the trachea. The pressure inside the trachea rises when air is injected through the SGAs. The pressure inside the trachea drops when air leakage occurred. This realizes a situation similar to the human respiratory system. The manikin was intubated with SGAs and air was injected into the airway. After that, the leakage was verified by the pressure fluctuation inside the airway.

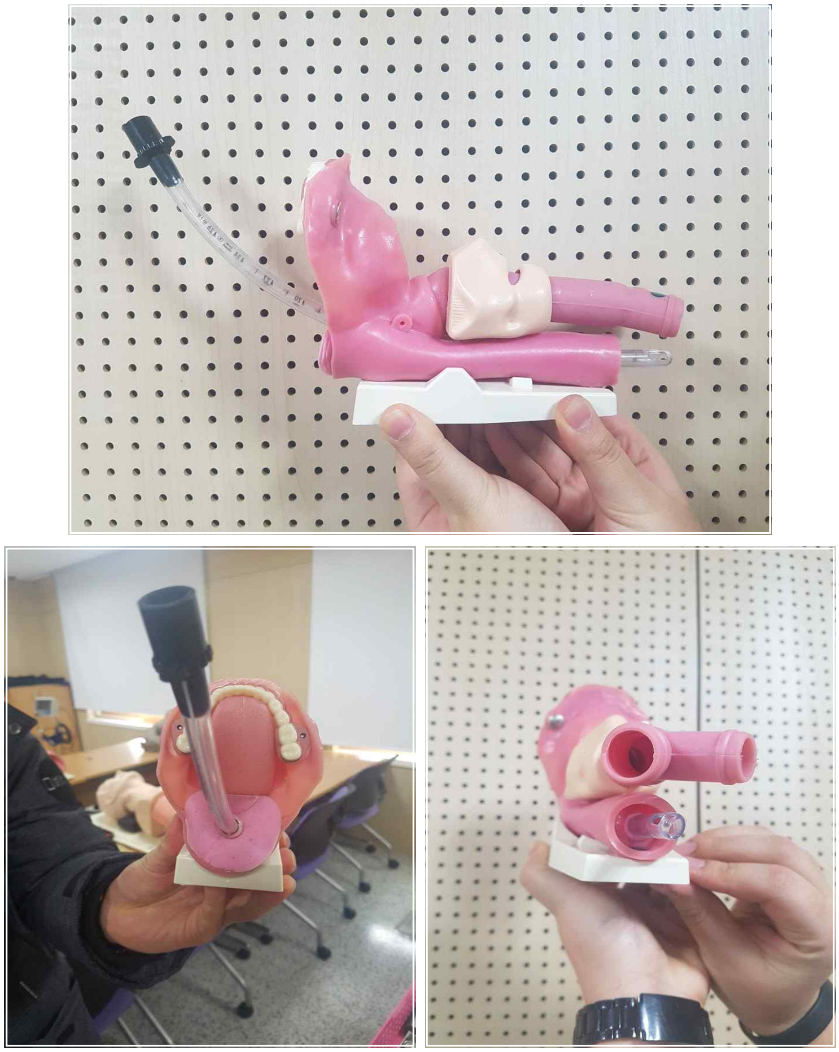

Figure 30. In-vitro performance evaluation about sealing.

Airway maintenance mannequins, shape and material are similar to real human respiratory system. Inside the mannequin, Sonogel was applied to achieve a similar viscosity to the surface of the actual respiratory system. The manikin was intubated with SGAs and air was injected into the airway. After that, the leakage was verified by the pressure fluctuation inside the airway.

2.4.2. In-vitro performance evaluation about pressure applied to the laryngeal lumen

The pressure applied by existing-, new-SGAs to the laryngeal lumen was measured and compared. FSR-400 pressure sensor (Interlink Electronics, California, USA) was installed in a diameter 40 mm circular acrylic tube simulating laryngeal lumen. The pressure applied to the acrylic plate was directly measured by intubating the cuffs [figure 31]. The voltage signals generated by the pressure sensors were converted to pressure values via an Arduino Mega 2560 (Arduino Inc., Italy). And the experiment was performed with the silicone cuff made by computerized tomography image of the existing-SGAs. Through this, the tension, elasticity and other factors of the cuff material were dispensed to analyze the difference according to the shape [figure 32, 33].

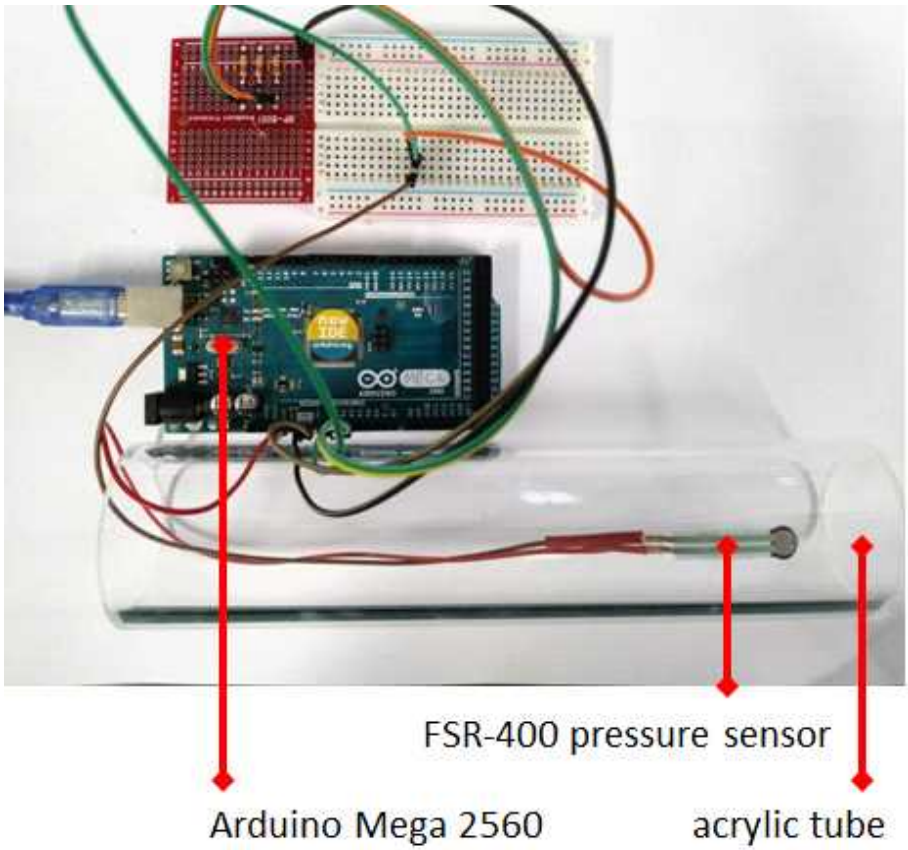

Figure 31. Pressure measuring system applied by SGAs cuff to the laryngeal lumen of the larynx.

FSR-400 pressure sensor was installed in a diameter 40 mm circular acrylic tube simulating laryngeal lumen. The voltage signals generated by the pressure sensors were converted to pressure values via an Arduino Mega 2560

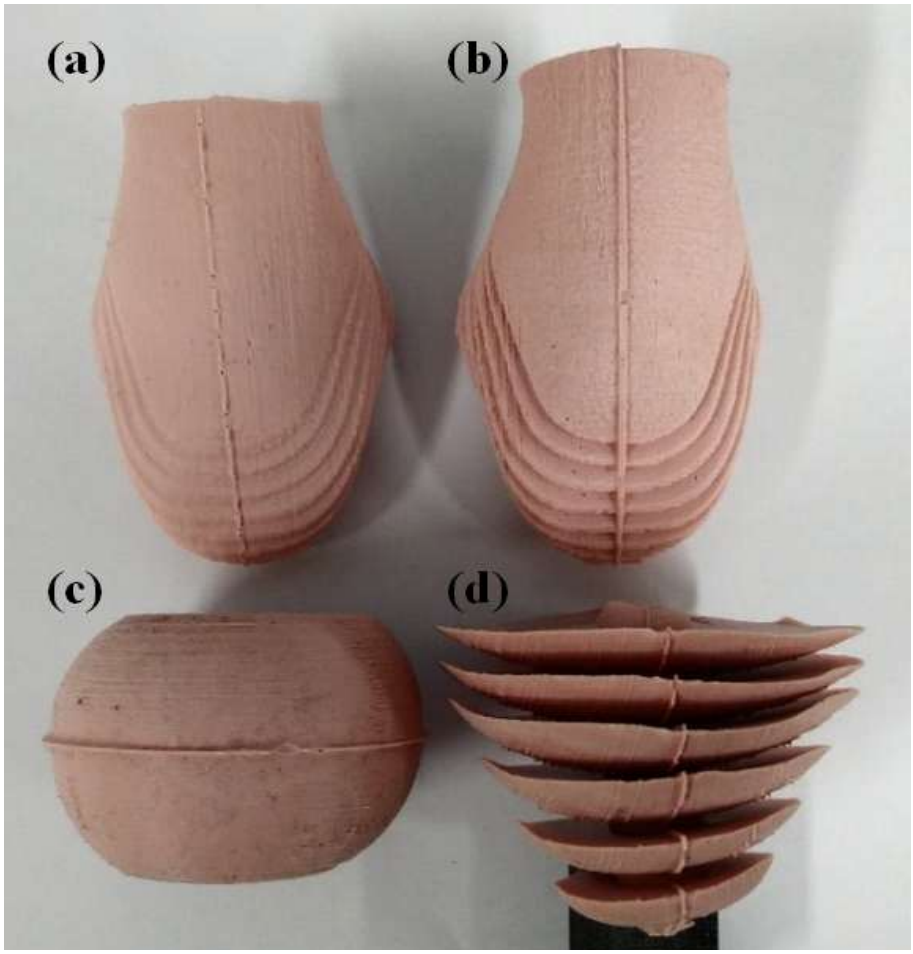

Figure 32. new-SGAs cuff and silicone cuff made by computerized tomography image of the existing-SGAs a) existing-IGEL cuff b) new-IGEL cuff c) existing-combitube proximal cuff d) new-combitube proximal cuff

Experiment was performed with the same shape of silicone cuff made by computerized tomography image of the existing-SGAs. Through this, the tension, elasticity and other factors of the cuff material were dispensed to analyze the difference according to the shape

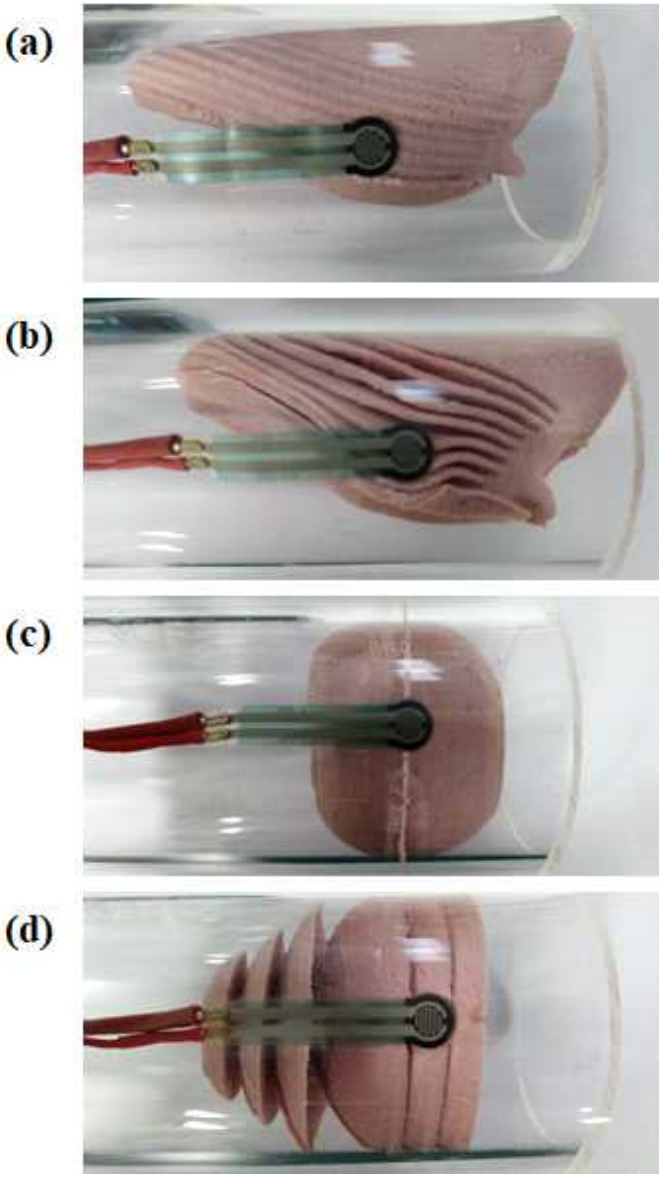

Figure 33. Measurement of pressure applied by new-SGAs to laryngeal lumen. a) existing-IGEL cuff b) new-IGEL cuff c) existing-combitube proximal cuff d) new-combitube proximal cuff

2.5. In-vivo performance evaluation of new-SGAs

We conducted in-vivo performance evaluation of new-SGAs by comparing the data from the SI with the data from the EI [figure 34]. The performance evaluation consisted of eight experimental groups according to the order of intubation of each SGAs, and one pig was assigned to each experimental group. Randomization was carried out to cross-test for each SGAs [figure 35]. The major data in this study are carotid arterial blood flow (mL / sec) and carotid arterial blood pressure (mmHg). After inducing cardiac arrest in the pigs, SGAs and e-tube were alternately intubated and the data was measured [figure 36]. The data measured in each SI section were averaged together with the data measured in the The EI section, which is the base section.

a)

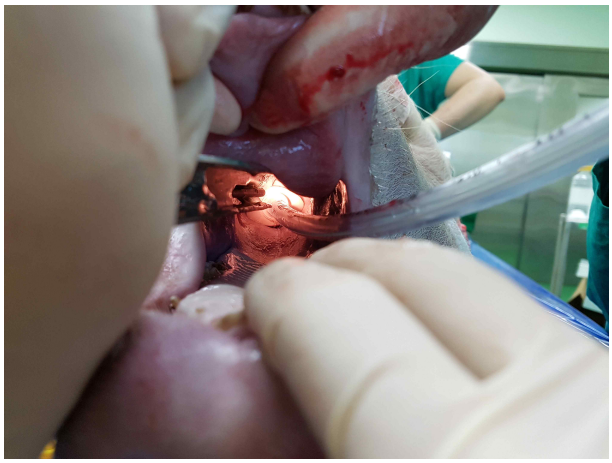

b)

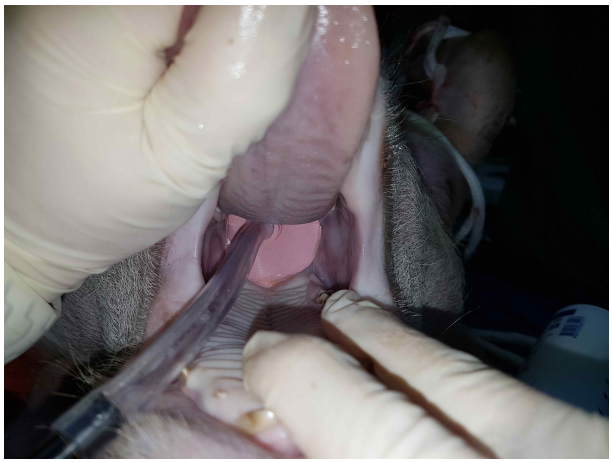

Figure 34. In-vivo performance evaluation of new-SGAs
a) new-IGEL b) new-combitube

	SGA#1	SGA#2	SGA#3	SGA#4
Group#1(one pig)	New-combitube	Existing-IGEL	Existing-combitube	New-IGEL
Group#2(one pig)	Existing-combitube	New-combitube	Existing-IGEL	New-IGEL
Group#3(one pig)	Existing-IGEL	New-combitube	New-IGEL	Existing-combitube
Group#4(one pig)	Existing-IGEL	New-IGEL	New-combitube	Existing-combitube
Group#5(one pig)	New-IGEL	Existing-IGEL	Existing-combitube	New-combitube
Group#6(one pig)	New-IGEL	Existing-combitube	Existing-IGEL	New-combitube
Group#7(one pig)	Existing-combitube	New-IGEL	New-combitube	Existing-IGEL
Group#8(one pig)	New-combitube	Existing-combitube	New-IGEL	Existing-IGEL

Figure 35. Classification of experimental group according to order of airway intubation

The preclinical study consisted of eight experimental groups according to the order of intubation of each SGAs, and one pig was assigned to each experimental group. Randomization was carried out to cross-test for each SGAs

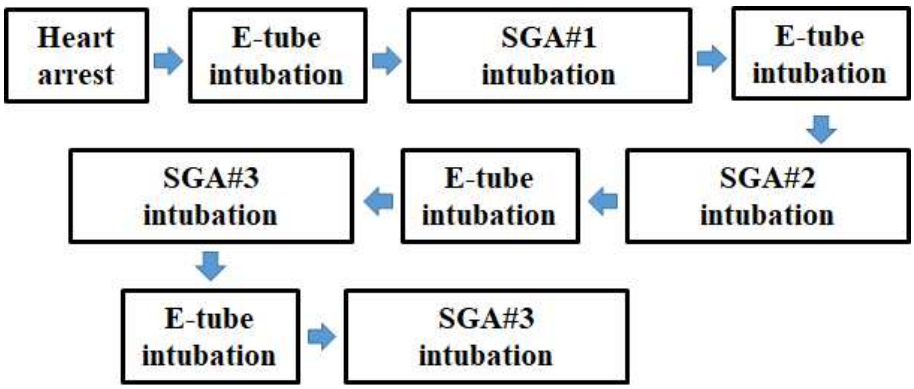

Figure 36. Performance evaluation research stage.

After inducing cardiac arrest in the pigs, SGAs and e-tube were alternately intubated to compare and analyze the data during EI and SI

Chapter 3. Result

3.1. Result of carotid blood flow on existing-SGA intubation using animal model

3.1.1. Result of carotid artery blood flow on LMA intubation using animal model

Table 1 shows the results of the carotid artery blood flow during LMA intubation. Table 2 shows comparison of changes in carotid artery blood flow between LMA intubation and EI (baseline). The change in carotid artery blood flow during SI was calculated as the percentage of EI interval. The results showed that the carotid blood flow per minute, mean carotid artery blood flow, mean carotid artery blood pressure, maximum carotid artery blood pressure decreased during LMA intubation. However, there was no statistically significant difference in consideration of significance probability.

Table 1. Analysis of carotid blood flow changes during LMA Intubation.

		E-tube(baseline)	LMA	Probability
Carotid blood flow per minute (mL/min)	Average/ Standard deviation	1699.0 / 295.3	1312.3 / 915.7	0.34
	Median/ Quadrant range	1657.1 / 1063.9 - 2554.0	1322.0 / 629.9 - 1667.7	0.42
Mean carotid artery blood flow (mL/sec)	Average/ Standard deviation	30.6 / 18.7	24.2 / 18.1	0.20
	Median/ Quadrant range	31.6 / 17.7 - 44.7	22.0 / 10.5 - 37.1	0.56
Maximum carotid artery blood flow (mL/sec)	Average/ Standard deviation	199.7 / 123.6	205.5 / 129.9	0.54
	Median/ Quadrant range	219.2 / 110.5 - 299.2	197.3 / 114.2 - 296.7	0.95
Minimum carotid artery blood flow (mL/sec)	Average/ Standard deviation	-89.4 / 67.0	-81.0 / 53.2	0.63
	Median/ Quadrant range	-72.3/ -135.9 - -46.4	-78.7 / -120.4 - -47.5	0.95
Mean carotid artery blood pressure (mmHg)	Average/ Standard deviation	14.4 / 13.3	13.4 / 15.4	0.43
	Median/ Quadrant range	12.6 / 4.7 - 21.6	9.2 / 2.5 - 19.7	0.69
Maximum carotid artery blood pressure (mmHg)	Average/ Standard deviation	56.5 / 17.4	55.2 / 21.5	0.44
	Median/ Quadrant range	54.8 / 43.4 - 72.8	53.1 / 42.8 - 66.1	0.77

Table 2. Comparison of changes in carotid artery blood flow between LMA intubation and EI (baseline)

	LMA			
	Average (%)	Standard deviation	Median (%)	Quadrant range
Carotid blood flow per minute (mL/min)	−9.0	46.3	−1.7	−44.5 − 5.0
Mean carotid artery blood flow (mL/sec)	−8.9	46.3	−1.0	−44.6 − 5.0
Maximum carotid artery blood flow (mL/sec)	7.5	24.2	0.4	−12.4 − 28.5
Minimum carotid artery blood flow (mL/sec)	9.5	37.7	14.6	−22.6 − 34.7
Mean carotid artery blood pressure (mmHg)	−19.7	41.8	−8.3	−35.7 − 1.9
Maximum carotid artery blood pressure (mmHg)	−4.0	14.0	−2.4	−11.5 − 2.1

3.1.2. Result of carotid artery blood flow on IGEL intubation using animal model

Table 3 shows the results of the carotid artery blood flow during IGEL intubation. Table 4 shows comparison of changes in carotid artery blood flow between IGEL intubation and EI (baseline). The change in carotid artery blood flow during SI was calculated as the percentage of EI interval. The results showed that the carotid blood flow per minute, mean carotid artery blood flow, maximum carotid artery blood flow, minimum carotid artery blood flow, maximum carotid artery blood pressure decreased during IGEL intubation. However, there was no statistically significant difference in consideration of significance probability.

Table 3. Analysis of carotid blood flow changes during IGEL Intubation.

		E-tube(baseline)	IGEL	Probability
Carotid blood flow per minute (mL/min)	Average/ Standard deviation	1860.1 / 1171.0	1491.4 / 1095.5	0.29
	Median/ Quadrant range	1589.1 / 1111.2 - 2784.4	1310.3 / 559.6 - 2399.9	0.42
Mean carotid artery blood flow (mL/sec)	Average/ Standard deviation	31.0 / 19.5	24.8 / 18.2	0.33
	Median/ Quadrant range	26.5 / 18.5 - 46.4	21.8 / 9.3 - 40.0	0.49
Maximum carotid artery blood flow (mL/sec)	Average/ Standard deviation	204.3 / 115.8	184.1 / 106.2	0.39
	Median/ Quadrant range	244.7 / 119.2 - 274.0	182.7 / 111.8 - 274.9	0.95
Minimum carotid artery blood flow (mL/sec)	Average/ Standard deviation	-81.6 / 51.9	-74.4 / 48.9	0.33
	Median/ Quadrant range	-88.3 / -104.2 - -44.8	-79.5 / -99.9 - -38.7	0.42
Mean carotid artery blood pressure (mmHg)	Average/ Standard deviation	16.3 / 15.4	14.2 / 12.8	0.31
	Median/ Quadrant range	15.3 / 5.7 - 27.3	15.5 / 7.6 - 22.2	0.73
Maximum carotid artery blood pressure (mmHg)	Average/ Standard deviation	57.2 / 22.4	55.0 / 21.1	0.27
	Median/ Quadrant range	63.2 / 40.0 - 74.9	61.6 / 39.3 - 72.2	0.53

Table 4. Comparison of changes in carotid artery blood flow between IGEL intubation and EI (baseline)

	IGEL			
	Average (%)	Standard deviation	Median (%)	Quadrant range
Carotid blood flow per minute (mL/min)	−18.6	28.0	−22.5	−32.9 – −1.6
Mean carotid artery blood flow (mL/sec)	−4.4	25.5	−6.5	−16.9 – 4.8
Maximum carotid artery blood flow (mL/sec)	−7.7	12.2	−4.4	−10 – −0.7
Minimum carotid artery blood flow (mL/sec)	−18.5	28.2	−22.4	−32.9 – −2.0
Mean carotid artery blood pressure (mmHg)	3.3	29.6	−1.9	−17.9 – 29.7
Maximum carotid artery blood pressure (mmHg)	−3.7	10.5	−4.1	−10.1 – 2.8

3.1.3. Result of carotid artery blood flow on combitube intubation using animal model

Table 5 shows the results of the carotid artery blood flow during combitube intubation. Table 6 shows comparison of changes in carotid artery blood flow between combitube intubation and EI (baseline). The change in carotid artery blood flow during SI was calculated as the percentage of EI interval. The results showed that the carotid blood flow per minute, mean carotid artery blood flow, maximum carotid artery blood flow, minimum carotid artery blood flow, mean carotid artery blood pressure, maximum carotid artery blood pressure decreased during combitube intubation. However, there was no statistically significant difference in consideration of significance probability.

Table 5. Analysis of carotid blood flow changes during combitube Intubation.

		E-tube(baseline)	Combitube	Probability
Carotid blood flow per minute (mL/min)	Average/ Standard deviation	1939.3 / 1283.5	1254.6 / 1348.8	0.22
	Median/ Quadrant range	2031.3 / 793.7 - 2308.9	862.5 / 324.8 - 1287.9	0.12
Mean carotid artery blood flow (mL/sec)	Average/ Standard deviation	32.3 / 21.4	20.9 / 22.5	0.22
	Median/ Quadrant range	33.9 / 13.2 - 38.4	14.4 / 5.4 - 21.4	0.12
Maximum carotid artery blood flow (mL/sec)	Average/ Standard deviation	223.3 / 143.2	195.9 / 124.5	0.62
	Median/ Quadrant range	232.2 / 109.9 - 299.6	205.4 / 96.5 - 276.4	0.60
Minimum carotid artery blood flow (mL/sec)	Average/ Standard deviation	-90.7 / 64.8	-73.5 / 49.9	0.48
	Median/ Quadrant range	-90.2 / -136.3 - -36.3	-77.2 / -105.0 - -37.5	0.53
Mean carotid artery blood pressure (mmHg)	Average/ Standard deviation	16.2 / 14.1	16.1 / 17.8	0.99
	Median/ Quadrant range	10.7 / 7.4 - 27.6	9.4 / 1.2 - 35.7	0.86
Maximum carotid artery blood pressure (mmHg)	Average/ Standard deviation	59.9 / 22.2	56.1 / 24.1	0.69
	Median/ Quadrant range	64.6 / 38.3 - 80.2	58.3 / 34.5 - 78.7	0.53

Table 6. Comparison of changes in carotid artery blood flow between combitube intubation and EI (baseline)

	Combitube			
	Average (%)	Standard deviation	Median (%)	Quadrant range
Carotid blood flow per minute (mL/min)	−42.0	34.5	−48.6	−74.3 −−16.5
Mean carotid artery blood flow (mL/sec)	−14.5	31.8	−18.7	−32 − 9.7
Maximum carotid artery blood flow (mL/sec)	−13.8	20.0	−12.0	−20.7 − 1.4
Minimum carotid artery blood flow (mL/sec)	−42.2	34.1	−48.6	−74.2 − −16.5
Mean carotid artery blood pressure (mmHg)	−70.7	218.5	−8.3	−39.8 − 3.9
Maximum carotid artery blood pressure (mmHg)	−8.0	14.1	−6.0	−14.7 − 0.6

3.2. Analysis of blood vessel shape using computed tomography image

3.2.1. Result of appearance analysis about laryngeal lumen 3D model

3D model of the laryngeal lumen of pigs intubated with LMA, IGEL, combitube and e-tube was made using a Seg3D and computed tomography images [figure 37, 38, 39, 40]

Figure 37 is a 3D model of trachea during EI. The cuff of the e-tube is intubated into the trachea. Thereafter, air is infused to inflate the cuff. Through this, the cuff is brought into close contact with the inner wall of the airway. As a result, the gap between the cuff and the inner wall of the trachea is blocked to achieve sealing between the trachea and the mechanical ventilator. The inflated cuff pressures the trachea. So, there is a gentle curvature in the middle part of the trachea. The e-tube does not apply pressure to the laryngeal lumen.

Figure 38 is the 3D model of laryngeal lumen during EI. It is identical to the laryngeal lumen before intubation which means unchanged laryngeal lumen. So, the 3D model is used as a control group to analyze the degree of change of the laryngeal lumen during SI.

Figure 39 is a 3D model of the laryngeal lumen during LMA intubation. Figure 40 is a 3D model of the laryngeal lumen during IGEL intubation. It can be seen that each of SGAs is well connected with the glottis. This confirms that the closed loop between the trachea

and the mechanical ventilation is well formed. **Figure 41** is a 3D model of the laryngeal lumen during combitube intubation. It shows that the distal cuff was successfully intubated through the esophagus. It can be seen that the distal cuff has expanded in the esophagus and the proximal cuff has expanded in the laryngeal lumen. This confirms that the closed loop between the trachea, the laryngeal lumen and the mechanical ventilation is well formed. Meshmixer was used to analyze changes in the medial length of the laryngeal lumen. The maximum internal diameter of the laryngeal lumen before the intubation is 20.2 mm. The maximum internal diameter of the laryngeal lumen during LMA intubation is 40.6 mm. The laryngeal lumen was expanded by 20.4 mm compared with the control group by LMA intubation. The maximum internal diameter of the laryngeal lumen during IGEL intubation is 39.5 mm. The laryngeal lumen was expanded by 19.3 mm compared with the control group by IGEL intubation. The maximum internal diameter of the laryngeal lumen during combitube intubation is 45 mm. The laryngeal lumen was expanded by 24.8 mm compared with the control group by combitube intubation.

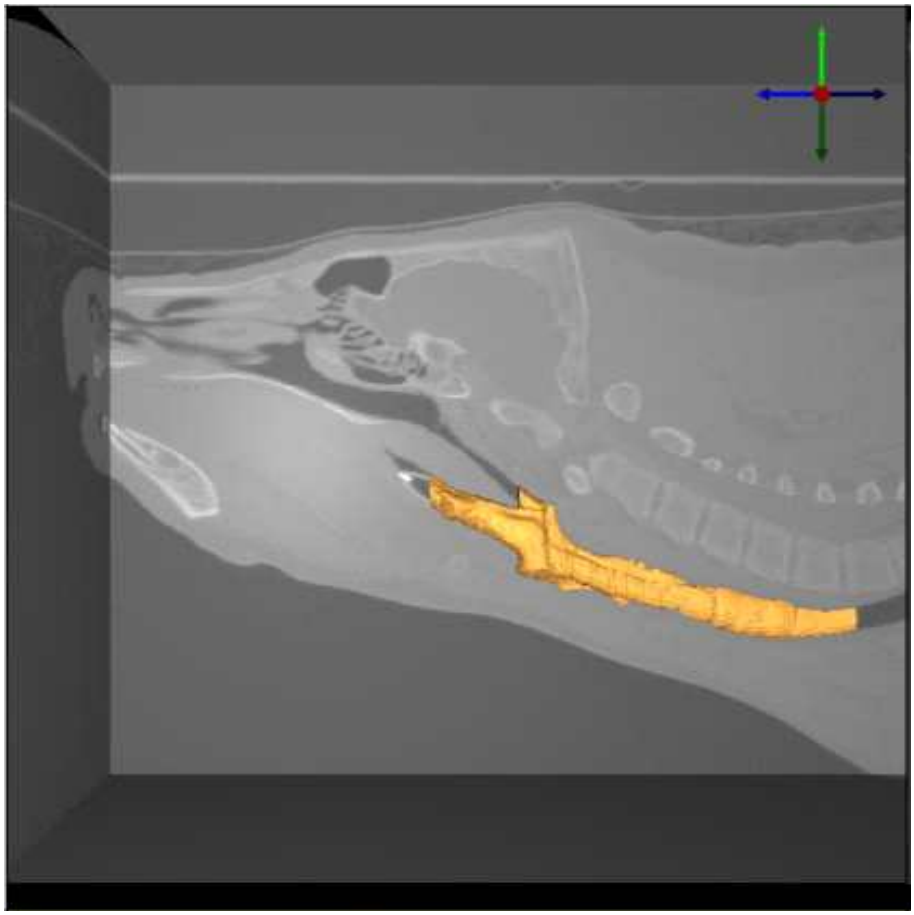

Figure 37. 3D model of trachea during EI

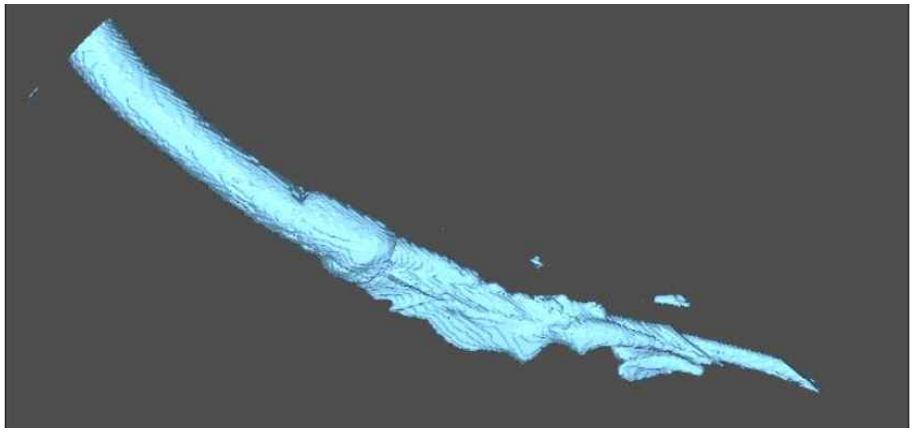

Figure 38. The 3D model of pork laryngeal lumen in the EI

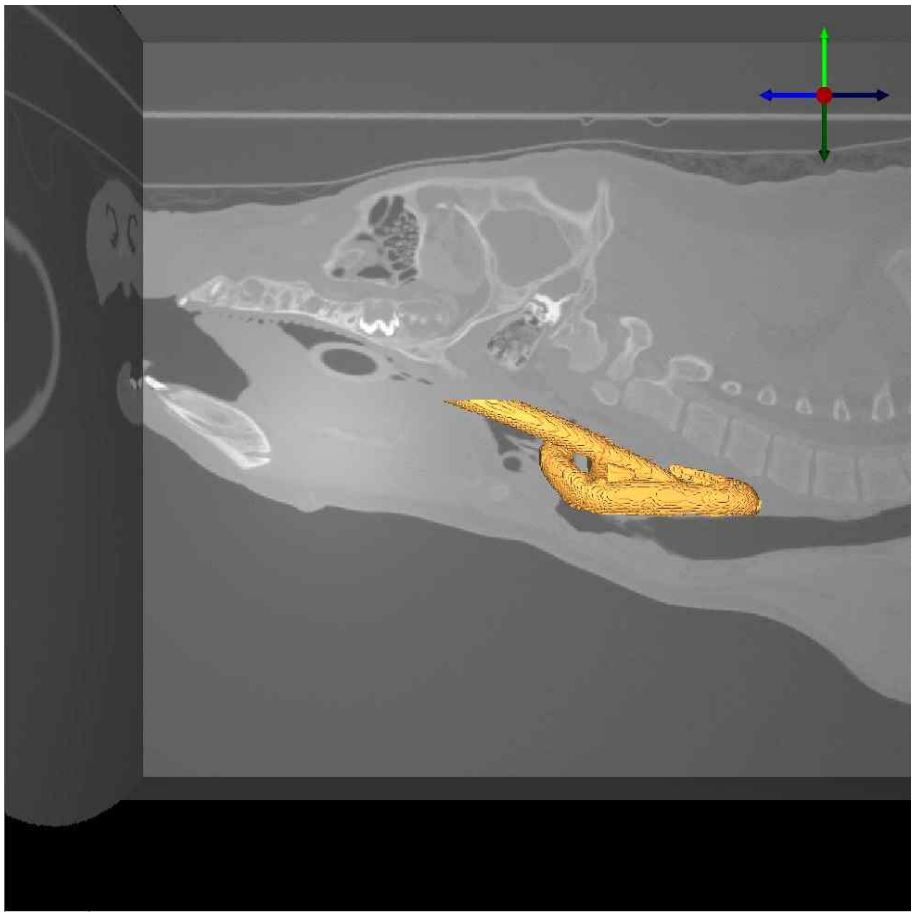

Figure 39. 3D model of the laryngeal lumen during LMA intubation

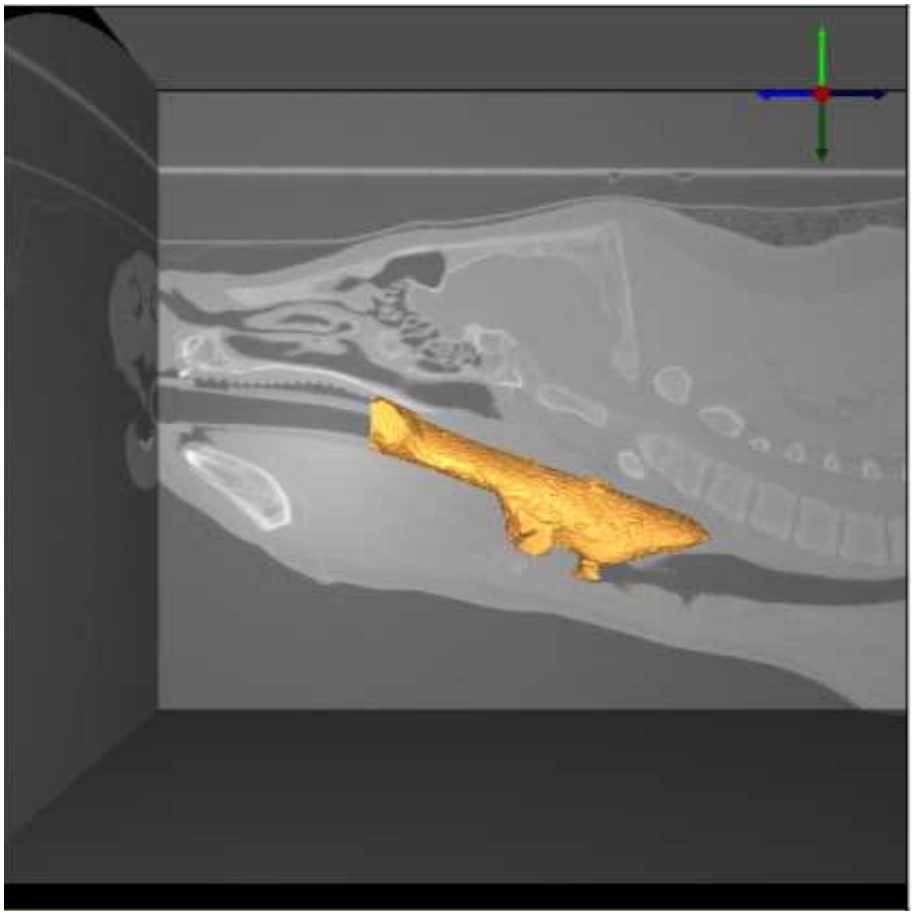

Figure 40. 3D model of the laryngeal lumen during IGEL intubation

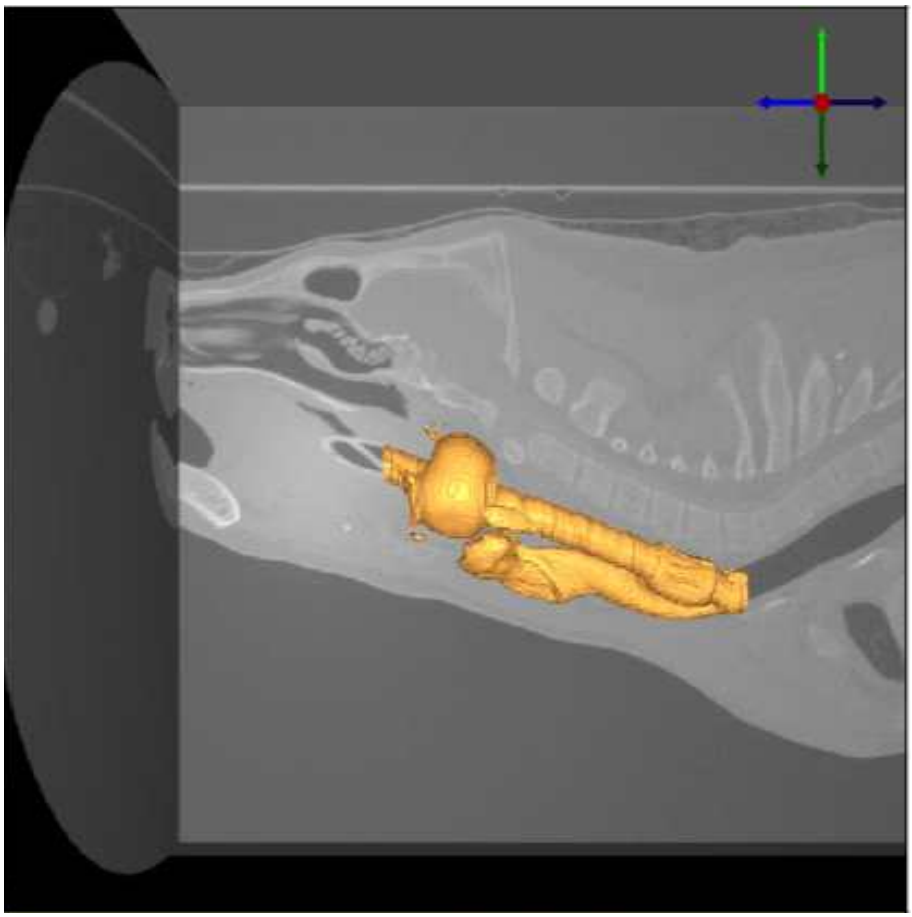

Figure 41. 3D model of the laryngeal lumen during combitube intubation

3.2.2. Result about appearance analysis of 3D model of SGAs before and after intubation

The 3D model of SGAs before and after intubation made by computerized tomography is shown in **figure 42, 43, 44**. **Figure 42** is LMA 3D model before and after intubation. **Figure 43** is IGEL 3D model before and after intubation. **Figure 44** is combitube 3D model before and after intubation. The change in diameter of each SGAs cuff were measured using a meshmixer. For the LMA, compression is up to 12.3 / 1.8 mm in width / height occurred. For the IGEL, compression is up to 7.5 / 0 mm in width / height occurred. For the combitube, compression is up to 11.4 / 8.0 mm in width / height occurred.

a) b)

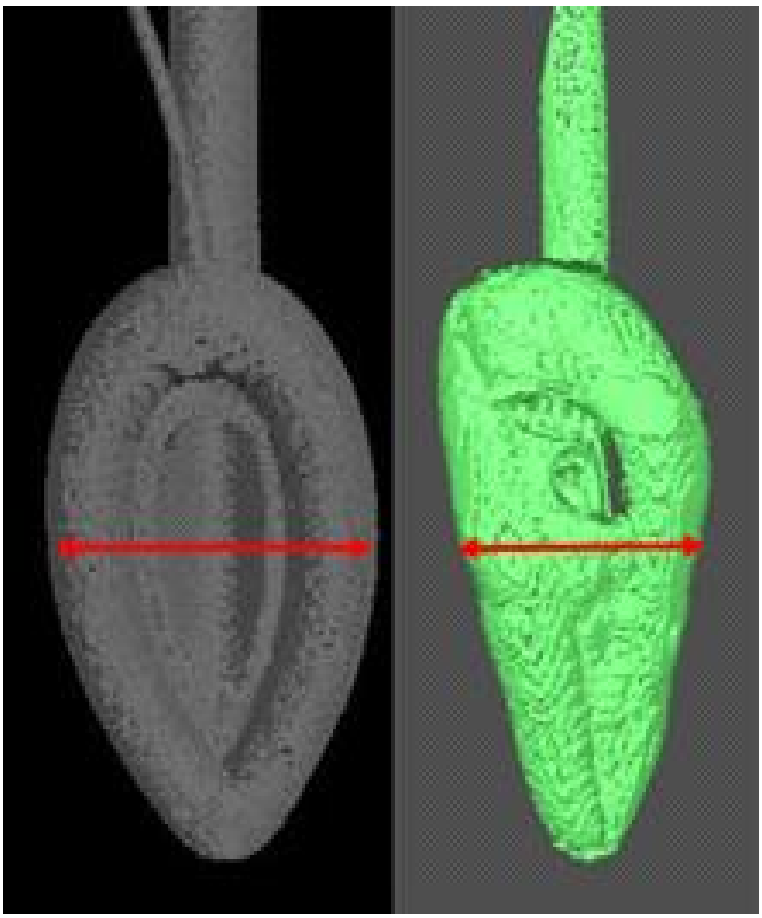

Figure 42. LMA 3D model a) before intubation b) after intubation

a) b)

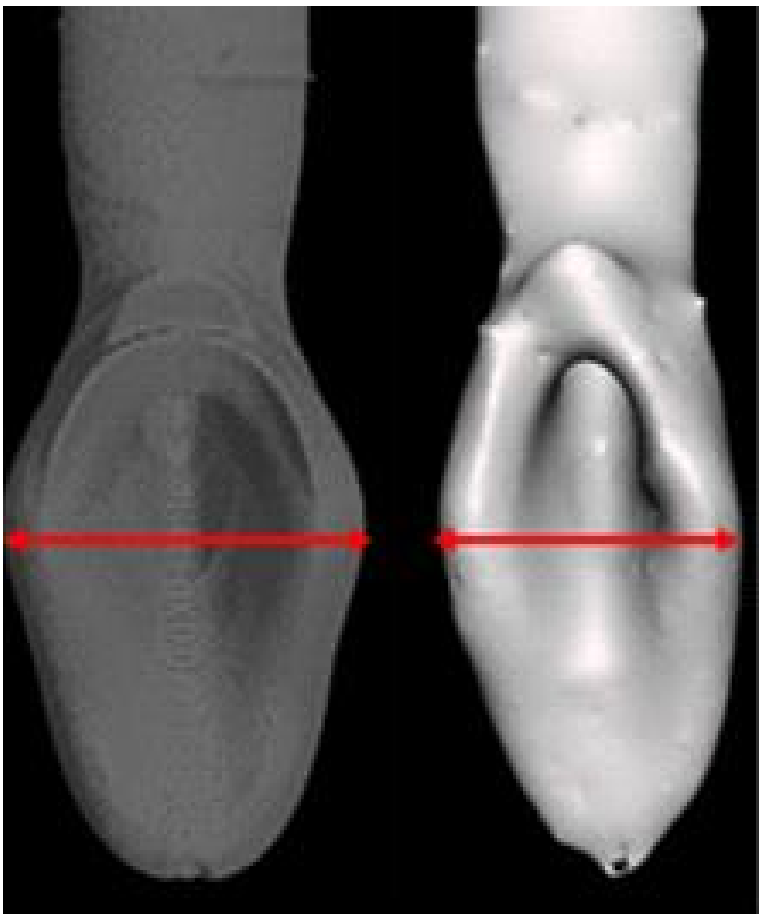

Figure 43. IGEL 3D model a) before intubation b) after intubation

a) b)

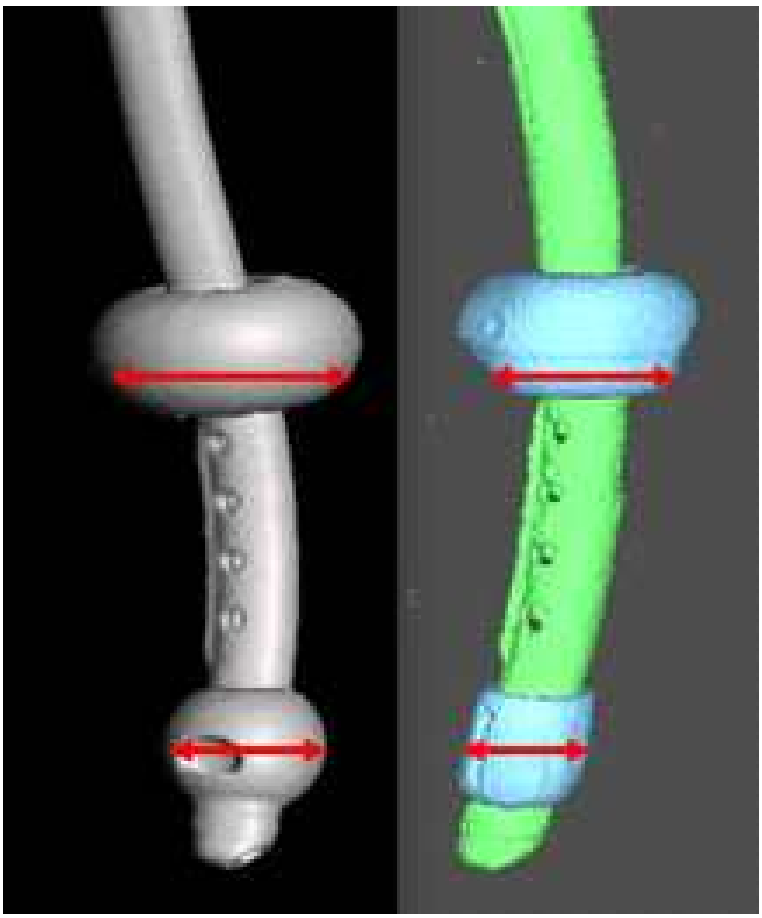

Figure 44. Combitube 3D model a) before intubation b) after intubation

3.2.3 Result about appearance analysis of carotid artery 3D model

The 3D model of carotid artery made by computerized tomography is shown in **figure 45, 46, 47, 48, 49. Figure 45** is Carotid artery 3D model during EI. **Figure 46** is Carotid artery 3D model during LMA intubation. **Figure 47,** is Carotid artery 3D model during IGEL intubation. **Figure 48, 49** is Carotid artery 3D model during combitube intubation. The flexion of the facial carotid artery, located around the cuff, was measured using a meshmixer. A maximum of 11.2 mm bending occurred in the facial carotid artery during LMA intubation. A maximum of 5.2 mm bending occurred in the facial carotid artery during IGEL intubation. A maximum of 10.0 mm bending occurred in the facial carotid artery during combitube intubation. **Figure 49** carotid artery during combitube intubation, the temporal carotid artery and the larynx carotid artery were collapsed due to the neck vertebrae.

Figure 45. Carotid artery 3D model during EI

Figure 46. Carotid artery 3D model during LMA intubation

Figure 47. Carotid artery 3D model during IGEL intubation

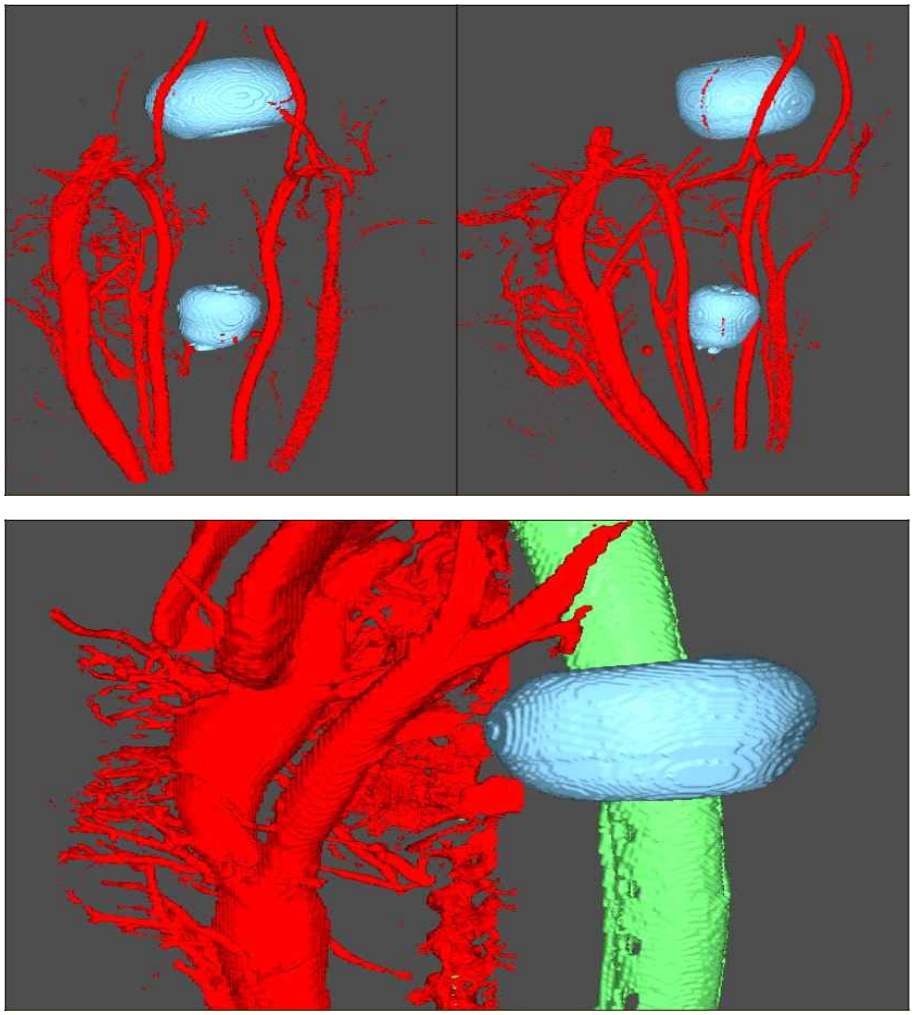

Figure 48. Carotid artery 3D model during combitube intubation

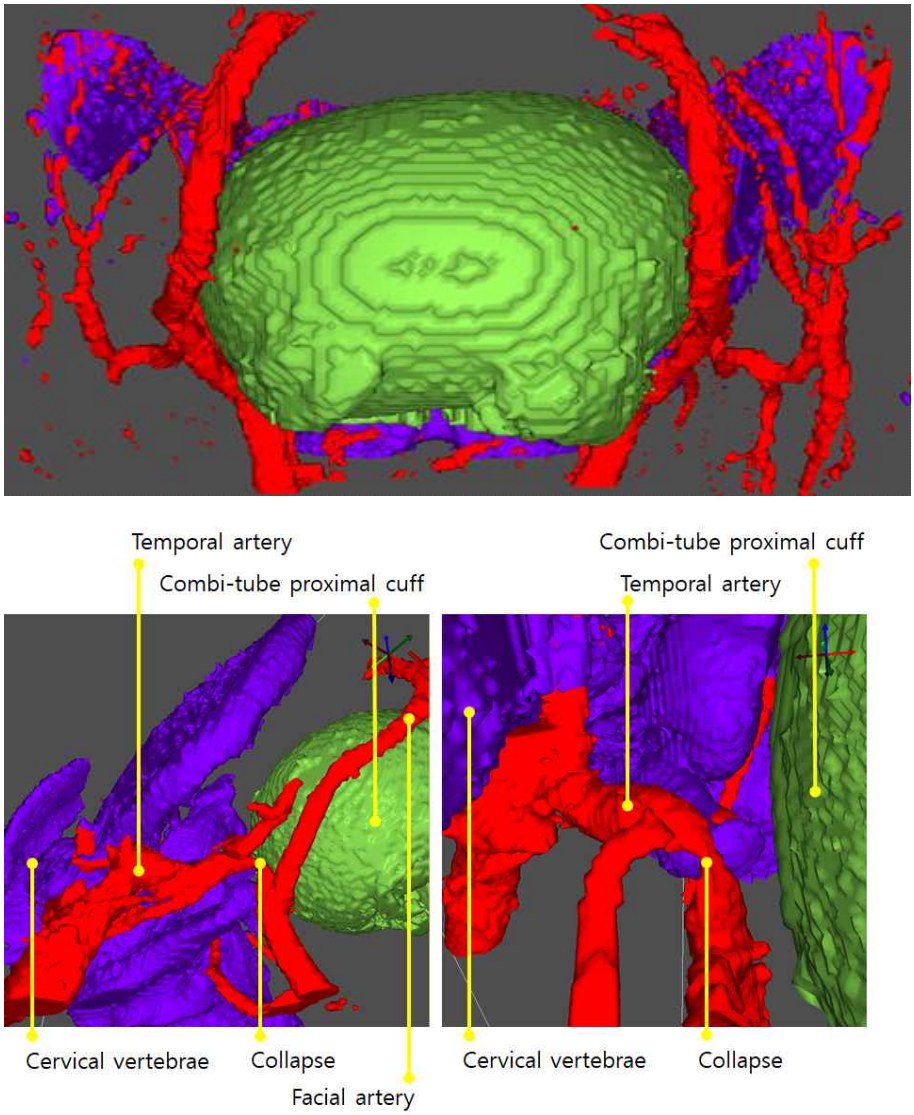

Figure 49. Collapsed carotid artery 3D model during combitube intubation

3.3. In-vitro performance evaluation of new-SGAs

First, the sealing performance of new-SGAs were verified by using the airway maintenance mannequins, shape and material are similar to real human respiratory system. As a result, air leakage did not occur in the new-LMA and new-combitube. We have verified the sealing performance of new-SGAs.

Second, the pressure applied by existing-, new-SGAs to the laryngeal lumen was measured and compared. The results are shown in Table 7. It was verified that the pressure applied to the laryngeal larynx by new-SGAs was low than existing-SGAs. The present study confirmed that the use of the developed glottic pneumoperitoneum can improve the blood flow and blood pressure reduction by reducing the pressure on the carotid artery.

Table 7. Result of In-vitro performance evaluation about pressure applied to the laryngeal lumen.

It was verified that the pressure applied to the laryngeal larynx by new-SGAs was low than existing-SGAs. The present study confirmed that the use of the developed glottic pneumoperitoneum can improve the blood flow and blood pressure reduction by reducing the pressure on the carotid artery.

	Pressure on laryngeal lumen (mmHg)	
	IGEL	Combitube
Existing	255	503
New	203	302

3.4. In-vivo performance evaluation of new-SGAs

Table 8 shows the results of the carotid artery blood flow during existing-IGEL intubation. The results showed that the carotid blood flow per minute, mean carotid artery blood flow, mean carotid artery blood pressure, maximum carotid artery blood pressure decreased during existing-IGEL intubation. Table 9 shows the results of the carotid artery blood flow during new-IGEL intubation. The results showed that the Carotid blood flow per minute, Mean carotid artery blood flow, Maximum carotid artery blood flow, decreased during new-IGEL intubation. Table 10 shows the results of the carotid artery blood flow during existing-combitube intubation. The results showed that the Carotid blood flow per minute, Mean carotid artery blood flow, maximum carotid artery blood flow, decreased during new-IGEL intubation. Table 11 shows the results of the carotid artery blood flow during new-combitube intubation. The results showed that the carotid blood flow per minute, mean carotid artery blood flow, maximum carotid artery blood flow, maximum carotid artery blood pressure decreased during new-IGEL intubation. However, there was no statistically significant difference in consideration of significance probability. Graph 1 summarizes the results of carotid flow rate. From the above graph, new-SGAs slightly reduces the carotid blood flow rate compared to existing-SGAs. This confirmed the improved tendency of the new-SGAs.

Table 8. Analysis of carotid blood flow changes during existing-IGEL Intubation

		E-tube(baseline)	Existing-IGEL	Probability
Carotid blood flow per minute (mL/min)	Average/ Standard deviation	876.4 / 699.4	656.3 / 732.6	0.58
	Median/ Quadrant range	546.5 / 320.4 - 1615.9	228.4 / 157.8 - 1346.9	0.41
Mean carotid artery blood flow (mL/sec)	Average/ Standard deviation	14.6 / 11.7	10.9 / 12.2	0.58
	Median/ Quadrant range	9.1 / 5.3 - 26.9	3.8 / 2.6 - 22.4	0.41
Maximum carotid artery blood flow (mL/sec)	Average/ Standard deviation	97.8 / 82.9	102.9 / 89.8	0.91
	Median/ Quadrant range	68.9 / 19.8 - 202.6	66.2 / 23.8 - 207.9	0.94
Mean carotid artery blood pressure (mmHg)	Average/ Standard deviation	9.7 / 11.2	4.8 / 7.8	0.33
	Median/ Quadrant range	5.2 / 1.3 - 18.2	3.6 / -2.1 - 9.9	0.25
Maximum carotid artery blood pressure (mmHg)	Average/ Standard deviation	52.1 / 26.6	42.1 / 24.4	0.45
	Median/ Quadrant range	46.5 / 32.2 - 74.1	45.2 / 18.7 - 59.7	0.53

Table 9. Analysis of carotid blood flow changes during new-IGEL Intubation

		E-tube(baseline)	New-IGEL	Probability
Carotid blood flow per minute (mL/min)	Average/ Standard deviation	845.3 / 700.4	707.1 / 785.5	0.73
	Median/ Quadrant range	1058.6 / 40.5 - 1489.4	562.5 / 11.8 -718.8	0.75
Mean carotid artery blood flow (mL/sec)	Average/ Standard deviation	14.1 / 11.7	11.8 / 13.1	0.73
	Median/ Quadrant range	17.6 / 0.7 - 24.8	9.4 / 1.9 - 12.0	0.75
Maximum carotid artery blood flow (mL/sec)	Average/ Standard deviation	115.3 / 102.5	106.8 / 91.8	0.87
	Median/ Quadrant range	77.6 / 44.9 - 183.5	73.2 / 47.4 - 153.9	0.95
Mean carotid artery blood pressure (mmHg)	Average/ Standard deviation	11.4 / 10.4	13.5 / 14.6	0.74
	Median/ Quadrant range	10.0 / 5.5 - 16.3	10.2 / 1.6 - 25.2	1.00
Maximum carotid artery blood pressure (mmHg)	Average/ Standard deviation	51.9 / 22.5	52.8 / 28.7	0.95
	Median/ Quadrant range	57.4 / 38.8 - 69.1	52.2 / 33.7 -69.4	0.83

Table 10. Analysis of carotid blood flow changes during existing-combitube Intubation

		E-tube(baseline)	Existing-combitube	Probability
Carotid blood flow per minute (mL/min)	Average/ Standard deviation	1083.5 / 752.9	803.4 / 652.2	0.47
	Median/ Quadrant range	1331.8 / 429.3 - 1758.1	720.2 / 165.9 - 1351.9	0.65
Mean carotid artery blood flow (mL/sec)	Average/ Standard deviation	18.1 / 12.5	13.4 / 10.9	0.48
	Median/ Quadrant range	22.2 / 7.2 - 29.3	12.0 / 2.8 - 22.7	0.65
Maximum carotid artery blood flow (mL/sec)	Average/ Standard deviation	119.6 / 97.9	111.7 / 98.4	0.88
	Median/ Quadrant range	111.4 / 47.6 - 171.1	77.0 / 39.7 - 178.7	0.85
Mean carotid artery blood pressure (mmHg)	Average/ Standard deviation	14.0 / 10.3	11.6 / 7.9	0.61
	Median/ Quadrant range	17.0 / 4.5 - 23.2	14.3 / 6.2 - 17.4	0.40
Maximum carotid artery blood pressure (mmHg)	Average/ Standard deviation	57.8 / 14.2	49.1 / 9.4	0.17
	Median/ Quadrant range	56.9 / 45.3 - 66.9	48.3 / 40.3 - 58.9	0.29

Table 11. Analysis of carotid blood flow changes during new-combitube Intubation

		E-tube(baseline)	New-combitube	Probability
Carotid blood flow per minute (mL/min)	Average/ Standard deviation	1135.9 / 1045.8	1018.3 / 911.5	0.82
	Median/ Quadrant range	1029.6 / 246.1 - 1701.4	837.3 / 113.9 - 1588.8	0.65
Mean carotid artery blood flow (mL/sec)	Average/ Standard deviation	18.9 / 17.4	16.9 / 15.2	0.82
	Median/ Quadrant range	17.2 / 4.1 - 28.4	13.9 / 1.9 - 26.5	0.65
Maximum carotid artery blood flow (mL/sec)	Average/ Standard deviation	118.3 / 96.8	113.6 / 105.0	0.93
	Median/ Quadrant range	103.8 / 28.9 - 185.9	87.5 / 41.3 - 185.3	0.85
Mean carotid artery blood pressure (mmHg)	Average/ Standard deviation	9.8 / 11.1	8.9 / 11.5	0.88
	Median/ Quadrant range	6.5 / 2.1 - 16.4	6.7 / 1.8 - 12.7	1.00
Maximum carotid artery blood pressure (mmHg)	Average/ Standard deviation	50.3 / 24.3	46.5 / 27.9	0.78
	Median/ Quadrant range	45.6 / 36.9-66.9	44.2 / 26.2 - 66.1	0.67

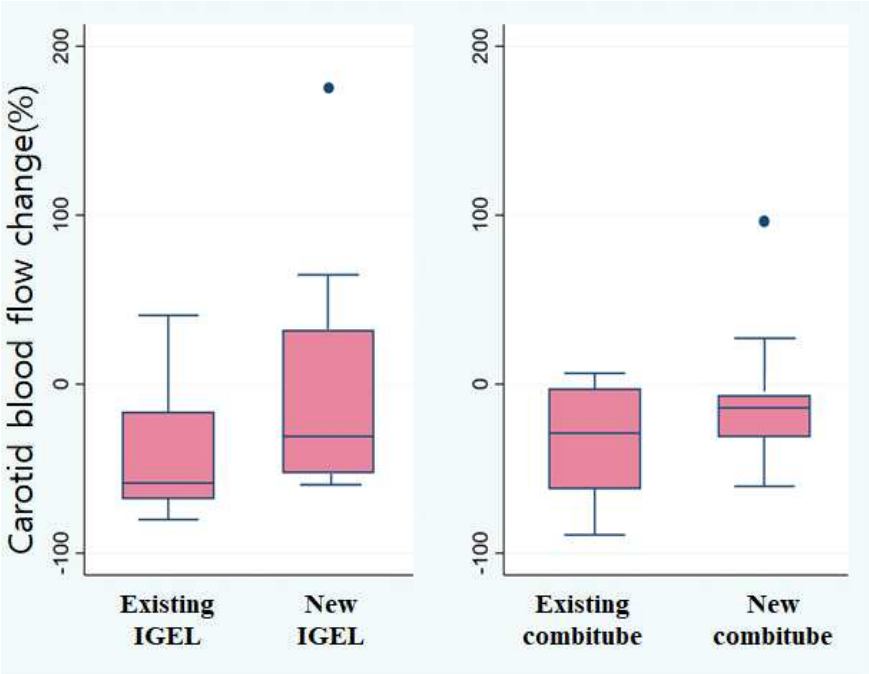

Graph 1. Result of in-vitro performance evaluation of new-SGAs

Chapter 4. Discussion

Supraglottic airway has the advantage that the required skill level is relatively low. Therefore, it is widely used as an alternative to EI in the field of medical practice [12]. However, in recent large-scale studies of cardiac arrest patients, the results of spontaneous circulation recovery, survival rate, and neurological prognosis are reported to be worse than those obtained with EI when using a SGA [15, 16]. In addition, in preclinical studies using the cardiac arrest model of pigs, it has been reported that carotid blood flow and pressure decreased during CPR [9, 10, 11]. The above phenomenon is presumed to be caused by pressing the carotid artery with the pressure applied to the laryngeal lumen by the cuff [6, 7, 12, 37]. In the above-mentioned large-scale study, the prognosis of the patient using the SGA was bad and the above effect is presumed to be the cause. The purpose of this study is as follows. First. identify the problems that arise in terms of hemodynamic aspects, especially brain survival, during EI. Second, analyze the causes of the problem. Third, develop the new-SGA to solve the problem.

4.1. Discussion of carotid blood flow on existing-SGA intubation using animal model

We conducted preclinical studies in order to identify the problems of the SGA by comparing the data from the SI with the data from the EI. For this purpose, we conducted preclinical studies using 12 pig heart cardiac arrest models for LMA, IGEL, combitube three types of SGA. As a result, carotid artery blood flow and pressure were decreased during LMA and combitube intubation. The carotid artery blood flow was decreased during IGEL intubation. This is consistent with the results of Segal N, Yannopoulos D, and Mahoney BD et al., Who statistically confirmed a significant reduction in carotid artery blood flow and pressure during a SGA intubation in a pig heart arrest model [12].

4.2. Discussion of blood vessel shape using computed tomography image

In order to analyze the cause of the problem of the SGAs, 3D models of SGAs, carotid artery and laryngeal lumen before and after intubation were prepared and then analyzed for appearance. The 3D model of the laryngeal lumen of pig before intubation and SGAs after intubation were output to FDM 3D printer.

4.2.1 Discussion of laryngeal lumen 3D model appearance analysis

3D model of the laryngeal lumen of pigs intubated with LMA, IGEL, combitube and e-tube was made using a Seg3D and computed tomography images [figure 37, 38, 39, 40]

Figure 37 is a 3D model of trachea during EI. The cuff of the e-tube is intubated into the trachea. Thereafter, air is infused to inflate the cuff. Through this, the cuff is brought into close contact with the inner wall of the airway. As a result, the gap between the cuff and the inner wall of the trachea is blocked to achieve sealing between the trachea and the mechanical ventilator. The inflated cuff pressures the trachea. So, there is a gentle curvature in the middle part of the trachea. The e-tube does not apply pressure to the laryngeal lumen.

Figure 38 is the 3D model of laryngeal lumen during EI. It is identical to the laryngeal lumen before intubation which means unchanged laryngeal lumen. So, the 3D model is used as a control group to analyze the degree of change of the laryngeal lumen during SI.

Figure 39 is a 3D model of the laryngeal lumen during LMA intubation. Figure 40 is a 3D model of the laryngeal lumen during IGEL intubation. It can be seen that each of SGAs is well connected with the glottis. This confirms that the closed loop between the trachea and the mechanical ventilation is well formed. Figure 41 is a 3D model of the laryngeal lumen during combitube intubation. It shows that the distal cuff was successfully intubated through the esophagus. It can be seen that the distal cuff has

expanded in the esophagus and the proximal cuff has expanded in the laryngeal lumen. This confirms that the closed loop between the trachea, the laryngeal lumen and the mechanical ventilation is well formed. Meshmixer was used to analyze changes in the medial length of the laryngeal lumen. The maximum internal diameter of the laryngeal lumen before the intubation is 20.2 mm. The maximum internal diameter of the laryngeal lumen during LMA intubation is 40.6 mm. The laryngeal lumen was expanded by 20.4 mm compared with the control group by LMA intubation. The maximum internal diameter of the laryngeal lumen during IGEL intubation is 39.5 mm. The laryngeal lumen was expanded by 19.3 mm compared with the control group by IGEL intubation. The maximum internal diameter of the laryngeal lumen during combitube intubation is 45 mm. The laryngeal lumen was expanded by 24.8 mm compared with the control group by combitube intubation. From the above results, it can be seen that the cuff of SGAs are putting a lot of pressure on the laryngeal lumen [40]. In addition, compression occurs in the carotid artery near the laryngeal lumen where pressure is applied. When the carotid artery is squeezed, the blood vessel cross section is reduced. The decrease in vessel cross-sectional area results in an increase in tube resistance. The increasing resistance increase energy consumption according to Darcy-Weisbach law. Also according to Hagen-Poiseuille's law, carotid blood flow and pressure are reduced.

4.2.2. Discussion about appearance analysis of 3D model of SGAs before and after intubation

The 3D model of SGAs before and after intubation made by computerized tomography is shown in **figure 42, 43, 44**. **Figure 42** is LMA 3D model before and after intubation. **Figure 43** is IGEL 3D model before and after intubation. **Figure 44** is combitube 3D model before and after intubation. The change in diameter of each SGAs cuff were measured using a meshmixer. For the LMA, compression is up to 12.3 / 1.8 mm in width / height occurred. For the IGEL, compression is up to 7.5 / 0 mm in width / height occurred. For the combitube, compression is up to 11.4 / 8.0 mm in width / height occurred. Through the above 3D model, it can be confirmed that many shrinkage occurred in each cuff. The contraction of the cuff is the result of an action reaction against the pressure exerted by the cuff on the laryngeal lumen. When the cuff inflates, the cuff exerts pressure on the laryngeal lumen. As a reaction to this, the laryngeal lumen compresses the cuff and causes contraction in the cuff. Therefore, it is possible to confirm the degree of pressure applied to the laryngeal lumen by the degree of contraction of the cuff in the 3D model. In the above 3D model, it is confirmed that the cuff has a lot of pressure on the laryngeal lumen because a large amount of contraction has occurred in the cuff. When the carotid artery is squeezed, the blood vessel cross section is reduced. The decrease in vessel cross-sectional area results in an increase in tube resistance and a higher energy consumption according to Darcy-Weisbach law. And according to Hagen-Poiseuille's law, carotid blood flow and pressure are reduced.

4.2.3. Discussion about appearance analysis of carotid artery 3D model

The 3D model of carotid artery made by computerized tomography is shown in **figure 45, 46, 47, 48, 49. Figure 45** is Carotid artery 3D model during EI. **Figure 46** is Carotid artery 3D model during LMA intubation. **Figure 47,** is Carotid artery 3D model during IGEL intubation. **Figure 48, 49** is Carotid artery 3D model during combitube intubation. The flexion of the facial carotid artery, located around the cuff, was measured using a meshmixer. A maximum of 11.2 mm bending occurred in the facial carotid artery during LMA intubation. A maximum of 5.2 mm bending occurred in the facial carotid artery during IGEL intubation. A maximum of 10.0 mm bending occurred in the facial carotid artery during combitube intubation. Through the above 3D model, it was proved that the pressure applied by the cuff to the laryngeal lumen actually presses the carotid artery. This is the same as a study of Michalek P, Donaldson W, Vobrubova E, Hakl M. and Nandwani N, Fairfield MC, Krarup K, Thompson Jl.that proved that the position and diameter of the carotid and jugular veins were changed during SGA intubation **[6, 14]**. Also, in **figure 49** carotid artery during combitube intubation, the temporal carotid artery and the larynx carotid artery were collapsed due to the neck vertebrae. This is due to the pressure exerted by the airway cuff, resulting in a collapse of the carotid artery, which is caught in the surrounding structures.. This causes an extreme decrease in the cross-sectional area of the carotid artery. When the carotid artery is squeezed, the blood vessel cross section is reduced. The decrease in vessel cross-sectional area results

in an increase in tube resistance. The increasing resistance increase energy consumption according to Darcy-Weisbach law. Also according to Hagen-Poiseuille's law, carotid blood flow and pressure are reduced. This is the same as preclinical results performed in this study.

4.3. Discussion of new-SGAs

In order to remedy the problems of the existing-SGAs, mechanical analysis is needed. First we analyze the principle of the sealing between the trachea and the ventilator. Second we analyze the principle of fixing to the laryngeal lumen by frictional force generated between the cuff and the laryngeal lumen. Third The principle of reducing the blood flow and blood pressure of the carotid artery by the pressure applied by the cuff to the laryngeal lumen was analyzed by Darcy-Weisbach law and Hagen-Poiseuille's law.

The new-SGA is designed with patents on ear plugs. The new-SGAs developed by applying the multi-flange cuff. Multi-flange cuff provide the following effects through the bending of thin plugs. First, it implements sealing between cuff and laryngeal lumen. Second, it reduces the pressure on the laryngeal lumen. When the SGA is inserted into the laryngeal lumen, pressure is applied to the thin plug. The pressure causes the thin plug to bend to fit the shape of the laryngeal lumen. A curved, thin plug closes the gap between the laryngeal lumen and the plug to create sealing. The pressure applied to the laryngeal lumen is reduced. However, the vertical drag decreases when the pressure applied to the laryngeal lumen

decreases. When the vertical drag decreases, the frictional force decreases and it is difficult to fix the new-SGAs. Generally, the frictional force of an object of the same weight is constant regardless of its contact area. However, if the contact surface is sufficiently wet or oil film, the frictional force is proportional to the area [39]. The laryngeal lumen surface is mucous, so the frictional force in the laryngeal lumen is proportional to the contact area. The bending of the thin plug increases the contact area between the laryngeal lumen and the plug to maintain the frictional force. Therefore, it is possible to maintain the frictional force by increasing the contact area while reducing the pressure applied to the luminal lumen.

The material of new-SGAs cuff was selected as silicon which is similar in material to rubber used in the existing-SGAs cuff and has low toxicity and low cost of materials. Therefore, 3D models of new-SGAs were constructed using Seg3D and Inventor (Professional 2016, Autodesk Inc., California, USA) [figure 25]. And 3D models of mold for casting silicon were designed using Meshmixer and Inventor [figure 26]. The molds were produced by FDM 3D printer [figure 27]. We fabricated the cuffs of new-SGAs by casting silicon on the mold [figure 28]. The new-SGAs were fabricated by inserting and fixing the cuffs on the e-tube

In vitro experiments were conducted to verify the performance of the new-SGAs. First, the sealing performance of new-SGAs were verified by using the airway maintenance mannequins. As a result, air leakage did not occur in the new-LMA and new-combitube. We have verified the sealing performance of new-SGAs. Second, the pressure applied by existing-, new-SGAs to the laryngeal lumen was

measured and compared [Table 7]. It was verified that the pressure applied to the laryngeal larynx by new-SGAs was low than existing-SGAs. The present study confirmed that the use of new-SGAs can improve the blood flow and blood pressure reduction by reducing the pressure on the carotid artery. We conducted in-vivo performance evaluation of new-SGAs by comparing the data from the SI with the data from the EI. As a result, new-SGAs slightly reduces the carotid blood flow rate compared to existing-SGAs. This confirmed the improved tendency of the new-SGAs.

Chapter 5. Conclusion

In recent large-scale studies of cardiac arrest patients, the results of spontaneous circulation recovery, survival rate, and neurological prognosis are reported to be worse than those obtained with EI when using a SGA. The above phenomenon is presumed to be caused by pressing the carotid artery with the pressure applied to the laryngeal lumen by the cuff. In the above-mentioned large-scale study, the prognosis of the patient using the SGA was bad and the above effect is presumed to be the cause. However, a clear basis for this has yet to be proven.

The purpose of this study is as follows. First. identify the problems that arise in terms of hemodynamic aspects, especially brain survival, during EI. Second, analyze the causes of the problem. Third, develop the new-SGA to solve the problem. In order to identify the problems in the carotid artery flow during supraglottic airway intubation (SI), preclinical studies are carried out on three kind of SGAs (LMA, IGEL, combitube) and e-tube by using 12 pigs heart arrest model. In this study, we compare the data during SI with the data during EI and identify the problems of SGA. As a result, it was confirmed that the carotid artery blood flow and pressure were decreased during SI. In order to analyze the cause of the problems during SI, three types of SGA and e-tube were implanted to pig and computed tomographic images are taken. After

making the 3D model of pre- and post-intubation SGA, carotid artery, laryngeal lumen by using the photographed images, we conduct the appearance analysis. Among these, 3D model of pre-intubation laryngeal lumen and post-intubation SGAs are output to 3D printer for more detailed appearance analysis. The results showed that the pressure applied to the laryngeal lumen by the SGAs cuff pressed the carotid artery. This resulted in flexion of the carotid artery, resulting in elongation of the blood vessel length and collapse of the artery, resulting in a decrease in the cross-sectional area of the blood vessel. Finally, the vascular resistance was increased and the carotid artery blood flow and blood pressure were reduced. Finally, we develop new-SGA to develop a new airway maintenance method which is most advantageous in terms of brain survival in cardiac arrest patients. To develop new-SGA, the first principle is to mechanically analyze the fixing principle of existing-SGA and the principle that the carotid artery is pressurized by the cuff to make hemodynamic difference. Secondly, the mechanistic viewpoints of the new-SGA that improve carotid artery blood flow and blood pressure decrease by reducing carotid artery pressure while maintaining airtightness are presented. Thirdly, the new-SGAs are produced, and conduct in vitro and in vivo performance evaluation. We have verified the sealing performance of new-SGAs through in vitro performance evaluation. In vitro performance evaluation has also shown that the new-SGAs reduces pressure on the laryngeal lumen. The results of the in-vivo performance evaluation showed new-SGAs improve carotid artery blood flow and pressure reduction.

Reference

[1] Hsia CCW, Dallas MH and Ewald RW. Lung structure and the intrinsic challenges of gas exchange. *Comprehensive Physiology*, 2016;6:827-895. doi: 10.1002/cphy.c150028

[2] Gilroy AM, MacPherson BR, and Ross LM. Atlas of anatomy. *Thieme* 2012:625-625.

[3] Pocock G, Richards CD and Richards DA. Human physiology. *Oxford university press* 2013:256-260

[4] Kacmarek RM, Dimas S and Mack CW. Essentials of Respiratory Care-E-Book. *Elsevier Health Sciences* 2013:196-199

[5] Netter FH. Atlas of Human Anatomy, 6th Edition. *Elsevier Health Sciences* 2014:312-322

[6] Nandwani N, Fairfield MC, Krarup K, Thompson J. The effect of laryngeal mask airway insertion on the position of the internal jugular vein. *Anaesthesia* 1997;52(1):77-79. doi: 10.1111/j.1365-2044.1997.012-az012.x

[7] Brenner DJ and Hall EJ. Computed tomography—an increasing source of radiation exposure. *New England Journal of Medicine* 2007 Nov;357:2277-2284. doi: 10.1056/NEJMra072149

[8] Dey TK, Edelsbrunner H and Guha S. Computational topology. *Contemporary mathematics* 1999;223: 109-144. doi: 10.1090/conm/223/03135

[9] Seeram E. Computed Tomography 4th edition. *Elsevier Health Sciences* 2015: 12-19.
[10] Chazelle B, Goodman JE and Pollack R, Advances in Discrete and Computational Geometry. *American Mathematical Soc*, 1999;223:251-255
[11] Cho A and Seok SH. Ethical Guidelines for Use of Experimental Animals in. *Journal of Bacteriology and Virology* 2013;43.1:18-26. doi: 10.4167/jbv.2013.43.1.18
[12] Segal N, Yannopoulos D, Mahoney BD et al. Impairment of carotid artery blood flow by supraglottic airway use in a swine model of cardiac arrest. *Resuscitation* 2012 Aug;83.8:1025-1030. doi: 10.1016/j.resuscitation.2012.03.025
[13] Oostrom H, Krauss MW and Sap R. A comparison between the v-gel supraglottic airway device and the cuffed endotracheal tube for airway management in spontaneously breathing cats during isoflurane anaesthesia. *Veterinary anaesthesia and analgesia* 2013;40.3:265-271. doi: 10.1111/vaa.12015
[14] Michalek P, Donaldson W, Vobrubova E and Hakl M. Complications associated with the use of supraglottic airway devices in perioperative medicine. *BioMed research international* 2015;2015: 746560. doi: 10.1155/2015/746560
[15] Wang HE, Szydlo D, Stouffer JA et al. Endotracheal intubation versus supraglottic airway insertion in out-of-hospital cardiac arrest. *Resuscitation* 2012;83.9:1061-1066. doi: 10.1016/j.resuscitation.2012.05.018
[16] Benoit JL, Gerecht RB, Steuerwald MT et al. Endotracheal intubation versus supraglottic airway placement in out-of-hospital cardiac arrest: a meta-analysis. *Resuscitation* 2015;93:20-26. doi: 10.1016/j.resuscitation.2015.05.007

[17] Debaty G, Shin SD, Metzger A et al. Tilting for perfusion: head-up position during cardiopulmonary resuscitation improves brain flow in a porcine model of cardiac arrest. *Resuscitation* 2015;87:38-43. doi: 10.1016/j.resuscitation.2014.11.019
[18] Corrado A and Gorini M. Negative-pressure ventilation: is there still a role?. *European respiratory journal* 2002;20.1:187-197. doi: 10.1183/09031936.02.00302602
[19] The NIH/NIGMS Center for Integrative Biomedical Computing. Seg3D Basic Functionality. http://www.sci.utah.edu/devbuilds/ seg3d_docs/Seg3DBasicFunctionality.pdf.(2017.10.01.)
[20] Bishop, Martin, et al. "Three-dimensional atrial wall thickness maps to inform catheter ablation procedures for atrial fibrillation. *Europace* 2015;18.3:376-383. doi: 10.1093/europace/euv073
[21] Augustin CM, Neic A, Liebmann M et al. Anatomically accurate high resolution modeling of human whole heart electromechanics: a strongly scalable algebraic multigrid solver method for nonlinear deformation. *Journal of computational physics*, 2016;305:622-646. doi: 10.1016/j.jcp.2015.10.045
[22] Zhao J, Kharche SR, Hansen BJ et al. Optimization of catheter ablation of atrial fibrillation: insights gained from clinically-derived computer models. *International journal of molecular sciences* 2015;16.5:10834-10854. doi: 10.3390/ijms160510834
[23] Wright M. Real-time atrial wall imaging. *Heart Rhythm* 2015;12.8:1836-1837. doi: 10.1016/j.hrthm.2015.04.038
[24] Wright M. Real-time atrial wall imaging. *Heart Rhythm* 2015;12.8:1836-1837. doi: 10.1061/40650(2003)4

[24] Magidson M and Dix D. Earplug. U.S. Patent No. 5,957,136. 28 Sep. 1999.
[25] Magidson M. Earplug. U.S. Patent No. 7,107,993. 19 Sep. 2006.
[26] Berg G and Lundblad N. Ear defender. U.S. Patent No. 5,249,309. 5 Oct. 1993.
[27] Leonard D. Detectable earplug. U.S. Patent No. 4,936,411. 26 Jun. 1990.
[28] Brown GO. The history of the Darcy-Weisbach equation for pipe flow resistance. *Environmental and Water Resources History* 2003. 34-43. doi: 10.1061/40650(2003)4
[29] Simpson A and Elhay S. Jacobian matrix for solving water distribution system equations with the Darcy-Weisbach head-loss model. *Journal of hydraulic engineering* 2010;137.6:696-700. doi: 10.1061/(ASCE)HY.1943-7900.0000341
[30] Von Bernuth RD. Simple and accurate friction loss equation for plastic pipe. *Journal of irrigation and Drainage engineering* 1990;116.2:294-298. doi: 10.1061/(ASCE)0733-9437(1990)116:2(294)
[31] Allen RG. Relating the Hazen-Williams and Darcy-Weisbach friction loss equations for pressurized irrigation. *Applied Engineering in Agriculture* 1996;12.6: 685-693. doi: 10.13031/2013.25699
[32] Sutera SP and Skalak R. The history of Poiseuille's law. *Annual Review of Fluid Mechanics* 1993;25.1:1-20. doi: 0066-4 189/93/0 115-0001
[33] Hellemans J, Forrez P and De Wilde R. Experiment illustrating Bernoulli's equation and Hagen-Poiseuille's law. *American Journal of Physics* 1980;48.3:254-255. doi: 10.1119/1.2342887

[34] McEwen WK. Application of Poiseuille's law to aqueous outflow. AMA archives of ophthalmology 1958;60.2:290-294. doi: 10.1001/archopht.1958.00940080306017
[35] Pirofsky B. The determination of blood viscosity in man by a method based on Poiseuille's law. *Journal of Clinical Investigation* 1953;32.4:292-298. doi: 10.1172/JCI102738
[36] Jagan NM. Biofluid Mechanics. *World Scientific* 1992: 41-78.
[37] Colbert S, O'Hanlon DM, Page R, et al. Haemodynamic changes with the laryngeal mask airway-off the cuff. *European journal of anaesthesiology* 1997;14.5:514-517. doi: 10.1046/j.1365-2346.1997.00182.x
[38] Silverman J, Suckow MA and Murthy S. The IACUC handbook. *CRC Press* 2014: 1-766
[39] Nave R., Hyper Physics, Mechanics, *National Science Teachers Association* 2001
[40] Gere JM and Goodno BJ. Mechanics of materials 7th. *Edn Google Scholar* 2009; 3-87

요약(국문초록)

경동맥 혈류 장애를 방지하는 성문위기도기의 개발

주윤하
서울대학교 대학원
협동과정 바이오엔지니어링 전공

성문위기도기는 기관과 인공호흡기 간 밀폐 루프를 형성하는 도구이다. 이는 요구되는 숙련도가 낮아서 기관내삽관의 대안으로 각광받고 있으며, 실제 의료 현장에서 광범위하게 사용되고 있다. 그러나 심혈관계 질환 환자에 대한 최근의 대규모 연구에서 성문위기도기 삽관이 기관내삽관 법보다 자발적 순환 회복, 생존율 및 신경학적 예후가 나쁘다는 결과가 지속적으로 보고되고 있다. 이는 성문위기도기를 삽관 후 커프스를 부풀릴 시 후두내강에 가해지는 압력이 경동맥을 압박하고, 이로 인해 경동맥 혈류가 방해되어 발생하는 문제점으로 추정된다. 그러나 이에 대해 명확한 근거는 아직 증명되지 않았다. 본 연구에서는 첫 번째로 성문위기도기 삽관 시 혈류역학적 측면, 특히 뇌 생존 측면에서 발생하는 문제점을 확인하고, 두 번째로 이러한 문제점이 발생하는 원인을 분석하며, 세 번째로 문제점을 개선하는 개발된 성문위기도기를 제작한다. 성문위기도기 삽관 시 발생하는 문제점을 확인하기 위해 후두마스크・아이겔・식도복합기도튜브 3종류의 성문위기도기를 대상으로 돼지 심정지 모델 12마리를 이용하여 전임상연구를 실시하였다. 그 결과 성문위기도기 3종류 모두에서 경동맥 혈류량 감소를 확인했고 2종류에서 혈압 감소를

확인했다. 성문위기도기가 경동맥 혈류에 영향을 미치는 원인을 분석하기 위해 삽관 전·후의 성문위기도기·경동맥·후두내강의 3D모델을 제작하고 외관분석을 실시하였다. 이를 위해 전임상연구용 돼지에게 기관내관과 성문위기도기 3종류를 번갈아 삽관하며 전산화단층촬영영상을 획득하였다. 그리고 획득한 영상과 Seg3D 및 Meshmixer를 이용하여 3D모델을 제작하고 외관분석을 실시하였다. 이 중 삽관 전 후두내강 및 삽관 후의 기도기 3D 모델을 FDM 3D프린터로 출력하여 좀 더 상세한 외관분석을 실시하였다. 그 결과 성문위기도기의 커프스가 후두내강에 많은 압력을 가한다는 것을 증명할 수 있었다. 이를 통해 후두내강에 가해지는 압력으로 경동맥이 압박되어 경동맥 혈류량 및 혈압이 감소되었음을 확인하였다. 마지막으로 앞에서 분석한 문제점을 개선하는 성문위기도기를 개발하였다. 이를 위한 첫 번째로 기존 성문위기도기의 기도와 인공호흡기간 밀폐를 구현하는 원리, 후두내강에 고정하는 원리, 커프스가 경동맥을 압박하여 경동맥 혈류량 및 혈압이 감소되는 원리를 역학적으로 분석하였다. 두 번째로 후두내강에 가해지는 압력은 줄이면서 밀폐를 유지하는 개발된 성문위기도기를 제시하고 그 원리를 역학적으로 분석하였다. 세 번째로 Inventor·Seg3D·Meshmixer로 설계하고 FDM 3D프린터로 출력한 거푸집에 실리콘을 주조하여 개발된 성문위기도기를 제작하였다. 네 번째로 새로 제작한 기도기를 대상으로 공기 누설 및 후두내강에 가하는 압력 측정 체외실험을 통해 성능평가를 실시하였다. 공기 누설 체외실험결과 개발된 성문위기도기 모두에서 공기 누설이 발생하지 않았고, 이를 통해 밀폐성능을 검증했다. 후두내강에 가하는 압력 측정 체외실험 결과 개발된 성문위기도기가 기존 성문위기도기에 비해 낮은 압력을 발생시켰다. 이를 통해 경동맥에 가해지는 압력을 줄여 경동맥 혈류량 및 혈압 감소를 개선할 수 있음을 검증했다. 최종적으로 돼

지 심정지 모델 8마리를 대상으로 체내실험을 실시하여 성능평가를 실시하였다. 그 결과 개발된 성문위기도기가 기존 성문위기도기보다 경동맥 혈류량 및 혈압 감소량이 작음을 확인했고, 이를 통해 문제점이 개선되었음을 확인했다.

주요어 : 성문위기도기, 전산화단층촬영영상 분석, 3D 모형 제작, 3D 프린팅
학 번 : 2016-21179